HAL open science

Citation: Differences in Cortical Structure and Functional MRI Connectivity in High Functioning Autism

Alessandra M Pereira, Brunno Campos, Ana C Coan, Luiz F Pegoraro, Thiago J R de Rezende, Ignacio Obeso, Paulo Dalgalarrondo, Jaderson C da Costa, Jean-Claude Dreher, Fernando Cendes

To cite this version:

Alessandra M Pereira, Brunno Campos, Ana C Coan, Luiz F Pegoraro, Thiago J R de Rezende, et al.. Citation: Differences in Cortical Structure and Functional MRI Connectivity in High Functioning Autism. Frontiers in Neurology, 2018, 9, 10.3389/fneur.2018.00539 . hal-02330965

HAL Id: hal-02330965

https://hal.science/hal-02330965

Submitted on 24 Oct 2019

HAL is a multi-disciplinary open access archive for the deposit and dissemination of scientific research documents, whether they are published or not. The documents may come from teaching and research institutions in France or abroad, or from public or private research centers.

L'archive ouverte pluridisciplinaire **HAL**, est destinée au dépôt et à la diffusion de documents scientifiques de niveau recherche, publiés ou non, émanant des établissements d'enseignement et de recherche français ou étrangers, des laboratoires publics ou privés.

frontiers in Neurology

ORIGINAL RESEARCH
published: 10 July 2018
doi: 10.3389/fneur.2018.00539

Differences in Cortical Structure and Functional MRI Connectivity in High Functioning Autism

*Alessandra M. Pereira[1,2], Brunno M. Campos[1], Ana C. Coan[1], Luiz F. Pegoraro[3], Thiago J. R. de Rezende[1], Ignacio Obeso[4,5], Paulo Dalgalarrondo[3], Jaderson C. da Costa[2,6], Jean-Claude Dreher[4] and Fernando Cendes[1]**

[1] Neuroimaging Laboratory, School of Medical Sciences, The Brazilian Institute of Neuroscience and Neurotechnology, University of Campinas, Campinas, Brazil, [2] Department of Pediatrics, Pontifícia Universidade Católica do Rio Grande do Sul, Porto Alegre, Brazil, [3] Department of Psychiatry, State University of Campinas, Campinas, Brazil, [4] Center for Cognitive Neuroscience, Reward and Decision Making Group, Centre National de la Recherche Scientifique, UMR 5229, Lyon, France, [5] Centro Integral en Neurociencias A.C., Hospital HM Puerta del Sur en Madrid, Madrid, Spain, [6] Brain Institute (InsCer), Pontifícia Universidade Católica do Rio Grande do Sul, Porto Alegre, Brazil

OPEN ACCESS

Edited by:
Argye Hillis,
Johns Hopkins Medicine,
United States

Reviewed by:
Elysa Jill Marco,
University of California, San Francisco,
United States
Roma Siugzdaite,
Ghent University, Belgium

***Correspondence:**
Fernando Cendes
fcendes@unicamp.br

Specialty section:
This article was submitted to
Applied Neuroimaging,
a section of the journal
Frontiers in Neurology

Received: 14 October 2017
Accepted: 18 June 2018
Published: 10 July 2018

Citation:
Pereira AM, Campos BM, Coan AC, Pegoraro LF, de Rezende TJR, Obeso I, Dalgalarrondo P, da Costa JC, Dreher J-C and Cendes F (2018) Differences in Cortical Structure and Functional MRI Connectivity in High Functioning Autism. Front. Neurol. 9:539. doi: 10.3389/fneur.2018.00539

Autism spectrum disorders (ASD) represent a complex group of neurodevelopmental conditions characterized by deficits in communication and social behaviors. We examined the functional connectivity (FC) of the default mode network (DMN) and its relation to multimodal morphometry to investigate superregional, system-level alterations in a group of 22 adolescents and young adults with high-functioning autism compared to age-, and intelligence quotient-matched 29 healthy controls. The main findings were that ASD patients had gray matter (GM) reduction, decreased cortical thickness and larger cortical surface areas in several brain regions, including the cingulate, temporal lobes, and amygdala, as well as increased gyrification in regions associated with encoding visual memories and areas of the sensorimotor component of the DMN, more pronounced in the left hemisphere. Moreover, patients with ASD had decreased connectivity between the posterior cingulate cortex, and areas of the executive control component of the DMN and increased FC between the anteromedial prefrontal cortex and areas of the sensorimotor component of the DMN. Reduced cortical thickness in the right inferior frontal lobe correlated with higher social impairment according to the scores of the Autism Diagnostic Interview-Revised (ADI-R). Reduced cortical thickness in left frontal regions, as well as an increased cortical thickness in the right temporal pole and posterior cingulate, were associated with worse scores on the communication domain of the ADI-R. We found no association between scores on the restrictive and repetitive behaviors domain of ADI-R with structural measures or FC. The combination of these structural and connectivity abnormalities may help to explain some of the core behaviors in high-functioning ASD and need to be investigated further.

Keywords: autism spectrum disorders, functional connectivity, MRI, cortical thickness, default mode network (DMN), social communication, stereotyped behavior

INTRODUCTION

Autism spectrum disorders (ASD) represent a complex group of neurodevelopmental conditions characterized by deficits in social behaviors, including both interpersonal social processes and self-referential thought (1). This condition is reported to affect 1 in 59 individuals according to the last CDC update of autism's estimated prevalence (2). The pathology of ASD is currently considered a disruption of brain development time-course with a wide range of heterogeneity among patients (3). The specific neurobiological substrates of this lifelong developmental disability remain unclear. Several studies reported a combination of structural abnormalities along with atypical brain connectivity in ASD (4–15). These abnormalities could help explain some of the symptoms of ASD and their severity.

Early investigations in ASD showed an increase in total brain volume at 2–4 years of age persisting into childhood but not adolescence (16). Some areas increase more than others, including frontal and temporal regions and the amygdala, while other structures present reduction in volume, such as the corpus callosum (17–26), probably indicating dysfunction of intra- and inter-hemispheric connectivity (15, 27–36). The first generation of studies using brain imaging failed to report consistent localized neocortical brain dysfunction (37, 38). However, structural neuroimaging has indicated various sites of anatomical abnormalities, providing some clues for a better understanding of this condition (17, 39–44).

Despite some inconsistencies, there is a trend from more recent studies which have observed regional increases of gray matter (GM) accompanied by local reductions of white matter (WM) (6, 38, 45). These findings support an increased local but reduced long-distance cortico-cortical reciprocal activity and functional coupling (46–48). Converging lines of evidence suggest that ASD is a complex disorder of brain connectivity (49, 50), involving aberrant functional connectivity (FC) within the default mode network (DMN), as well as between the DMN and several cortical and subcortical areas (13, 15, 27, 30, 31, 34–36, 44, 51–70, 107, 135).

The DMN is a set of structures known to be particularly engaged when participants are at rest **(Figure 1)**. Anatomically, this network consists of the posterior cingulate cortex (PCC), retrosplenial cortex, lateral parietal/angular gyrus, medial prefrontal cortex, superior frontal gyrus, regions of the temporal lobe, and the parahippocampal gyrus (54, 71–73, 79). Many have speculated that the DMN function may extend beyond cognitive processes and encompass the role of maintaining homeostasis between excitatory and inhibitory neuronal responses (74, 75). Others have argued that it is active when contemplating scenarios and events, when the mind is wandering, or when conducting lower-level observations of the individual's external surroundings (76–79). More recently, the "developmental disconnection model," proposed by many authors, links the core symptoms of ASD to weak FC between remote cortical regions and an excess of FC within local regions (80–82). For recent reviews in the topic see references (6, 15, 37, 43, 44, 50, 57, 67, 83–86).

It is currently unclear the extent of regions overlap between abnormal structural and functional connectivity in ASD patients and its relationship with different clinical presentations in the spectrum of this condition (26, 87, 88). The understanding of the relationship between structural and functional alterations is also compromised by the high heterogeneity of individuals and the age-related differences reported among different ASD groups (26). The comparison between brain structure and function in a single group of ASD individuals with similar phenotypic pattern can shed light on these complex interactions and establish a link with clinical symptomatology in these patients.

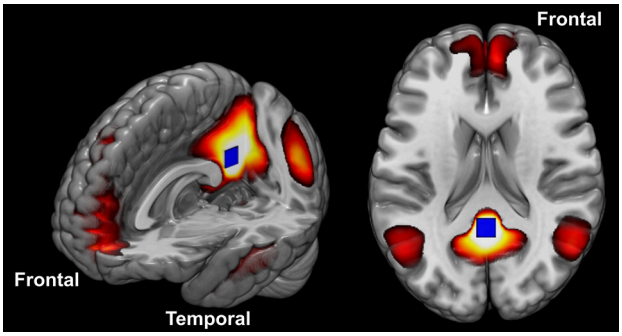

FIGURE 1 | The DMN constituent components. The blue square placed in the posterior cingulate cortex illustrates the seed position described in the methods.

We aimed to characterize the relationships between structural and functional abnormalities in a cohort of patients with high-functioning autism. We performed a high resolution multimodal structural (cortical thickness, gyrification index, surface area and GM volume) and functional (resting-state FC) analysis to detect superregional, system-level alterations attempting to establish a neurobiological foundation to pathology and clinical symptoms in this part of the spectrum of autism—adolescents and young adults with high-functioning autism without associated depression, psychosis, seizures, or other major psychiatric disorders.

METHODS

Participants

We recruited 22 adolescents and young adults with ASD and 29 normal controls from the local community and the University of Campinas. This study was approved by the Ethics Committee of the University of Campinas (plataformabrasil.saude.gov.br; reference number: CAAE 02388012.5.0000.5404; number of the approved ethical statement: 190409). All participants provided written informed consent approved by the Ethics Committee. For the participants younger than 18 years of age, we obtained informed consent from parents or guardians, as well as from the participants themselves.

A trained and qualified clinician made the diagnosis of ASD using the DSM-5 criteria after interviewing the family and examining each patient. A second investigator confirmed the diagnosis using the "Current" Scores of the Autism Diagnostic Interview-Revised (ADI-R) (89). The ADI-R is a clinical

diagnostic instrument for assessing autism in children and adults (89). The ADI-R provides a diagnostic algorithm for autism as described in both the ICD-10 and DSM-IV and is one of the most important validated ASD measures available in Brazil. The clinician's observation provides the opportunity to put the patient's behavior into the context of knowledge about other patients, but information from caregivers provides a broader context needed in understanding the patient's day to day behavior in a wide range of situations, his or her history, as well as family expectations, resources, and experiences and other important contextual factors. Thus, patient's testing and parent interviews should be viewed as complementary and necessary components of the diagnostic evaluation after the clinical evaluation and DSM-5 criteria. All patients were required to have a full-scale IQ greater than 85, as measured by the Wechsler Abbreviated Scale of Intelligence.

Exclusion criteria comprised a history of major psychiatric disorders (e.g., depression, psychosis), seizure, head injury, toxic exposure, facial dysmorphic features, and the evidence of genetic, metabolic, or infectious disorders. We also excluded individuals with secondary autism related to a specific etiology such as tuberous sclerosis or Fragile X syndrome (all included patients had a negative investigation of tuberous sclerosis and Fragile X syndrome).

Thirteen individuals in the ASD group were using a variety of psychoactive medications. Nine subjects were not under psychoactive drug treatment. Five subjects were taking psychostimulants, seven were taking antipsychotics, and six were taking selective serotonin reuptake inhibitors (SSRIs) for anxiety and compulsive behaviors. Six of these subjects were using more than one of the medications listed above. Participants were instructed not take any medication 1 day before their visit.

Neuroimaging Data Acquisition

We acquired functional and structural MRIs on a 3T scanner (Phillips, Achieva; Best, The Netherlands) with the following protocol:

- Resting-state fMRI: 6 min echo-planar images (EPIs), 180 dynamics, voxel size = $3 \times 3 \times 3$ mm^3, 40 slices, no gap, FOV = $240 \times 240 \times 120$ mm^3, TE = 30 ms, TR = 2,000 ms, flip angle = 90°. For this specific acquisition, we instructed all individuals to keep their eyes closed, not to fall asleep and try not to move for the duration of the scan. We used memory foam pillows placed around the participant's head to minimize head movement.
- Structural MRI: Volumetric T1-weighted images acquired on the sagittal plane, voxel size = $1 \times 1 \times 1$ mm^3, no gap, TR = 7 ms, TE = 3.2 ms, flip angle = 8°, FOV = $240 \times 240 \times 180$ mm^3. The number of slices varies with the size of the head, with an average of 160 sagittal slices.

MRI sequences were corrected for gradient non-linearity during the reconstruction step in the Phillips scanner. We performed a visual inspection of all structural and functional images to assess image quality, movement artifacts, and the existence of clinically relevant abnormalities.

Image Processing and Analysis

Our MRI phenotyping combined group- and individual-level analysis of GM volume, cortical thickness and folding complexity, which are three established *in vivo* markers of brain morphology and development. There was no difference between the groups on movement in the scanner for the structural imaging.

Voxel-Based Morphometry Analysis

We performed VBM with the VBM8/SPM8 toolbox (Wellcome Department of Cognitive Neurology, http://www.fil.ion.ucl.ac.uk) for detection of GM volume abnormalities. VBM allows the automated identification of the whole brain GM differences between groups (90). Post-processing of the T1-weighted images included normalization to the same stereotaxic space (MNI-152 template), modulation and segmentation of the images into GM, WM and cerebrospinal fluid (CSF). The DARTEL algorithm was included to increase the accuracy of the alignment between subjects (91). The resultant GM images were smoothed with a 10 mm FWHM isotropic Gaussian kernel. We excluded eight outliers (four ASD patients and four controls) detected in a quality test for image homogeneity and co-registration. Therefore, the final VBM analysis included 19 ASD patients and 25 controls (all other analyses from here on included the 22 patients and 29 controls).

We used two-sample *t*-tests (to adjust for multiple comparisons we considered a $p < 0.001$, minimum of 30 contiguous voxels) to search for areas of volume reduction or increase in ASD patients. First, we looked for areas of GM volume reduction or increase in the ASD group with age as covariable. As a second approach, we looked at the differences between groups in the correlation between age and GM volumes with total IQ as a covariate.

Cortical Thickness, Surface Area, and Gyrification Analysis With FreeSurfer

We performed cortical reconstruction and volumetric segmentation with the FreeSurfer image analysis suite (http://surfer.nmr.mgh.harvard.edu/), which is a well-validated method already described in previous publications (92–94). A single filled WM volume was generated for each hemisphere after intensity normalization, skull stripping, and image segmentation using a connected components algorithm. A surface tessellation was generated for each WM volume by fitting a deformable template. This resulted in a triangular cortical mesh for GM and WM surfaces in each hemisphere. Cortical thickness, then, was calculated as the shortest distance between GM and WM surfaces. Vertex-wise measurements of surface area were determined as the area of a vertex on the GM surface (5). We used the FreeSurfer default Gaussian filter of 10 mm FWHM to smooth the surfaces (92, 94).

Another volumetric measure obtained from FreeSurfer is the local gyrification index (LGI) which was developed by Schaer et al. (95). The LGI was defined as the ratio between the GM surface border and an outer border in successive coronal sections (96). To calculate this LGI, FreeSurfer uses both tessellated outer and inner contours of the pial surface, which were covered by a

triangle mesh. For each vertex on the outer surface, a spherical region of interest is created with a standard size of 25 mm radius. Therefore, the LGI is given as the ratio between the outer area on the surface and the area comprehended in the real pial surface (95). Thus, the LGI for each vertex on the pial surface reflects the amount of cortex buried in its locality. The LGI values obtained were mapped onto a normalized cortical surface.

We then compared regional cortical thickness, surface area and gyrification index between autism and control groups using a general linear model (GLM) with age and total IQ as covariates. To correct for multiple comparisons, we performed a cluster-based correction (level of significance at $\alpha = 0.01$) (97).

ROI Analysis With Data Extracted From FreeSurfer

ROI measures of cortical thickness, cortical area and LGIs for 33 gyral regions generated by FreeSurfer (98, 99) (https://surfer.nmr.mgh.harvard.edu/fswiki/FsTutorial/AnatomicalROI#Groupstatsfiles) were corrected for total intracranial volume generated by FreeSurfer and exported to SPSS Statistics version 20 (IBM Corp. Released 2011. IBM SPSS Statistics for Windows, Version 20.0. Armonk, NY: IBM Corp.).

Group differences in gyral-level cortical thickness, cortical area, and LGIs were analyzed using mixed GLMs with diagnosis (autism vs. controls) as the between-subjects factor, the 33 gyral regions from both hemispheres (98, 99) as the within-subjects factors, also with age and total IQ as covariates. We also ran the same mixed GLM for subcortical volumes generated by FreeSurfer. All comparisons between controls and patients were Bonferroni corrected for multiple comparisons.

Resting-State Functional MRI Processing and Analysis

To perform the resting-state processing and analysis, we used the UF^{2}C (User-Friendly Functional Connectivity; https://www.lniunicamp.com/uf2c) toolbox (100) on a PC running MATLAB 2013a (The MathWorks, Inc., Natick, MA, USA) with SPM8 (Wellcome Trust Centre for Neuroimaging). The UF^{2}C toolbox (100) pipeline started with a standard image preprocessing protocol which includes: (i) functional realignment to the mean image (movement parameters are saved); (ii) structural-functional co-registration; (iii) structural segmentation into GM, WM and CSF tissues; (iv) functional and structural normalization (MNI 152); (v) functional image smoothing (kernel with double voxel sizes $= 6 \times 6 \times 6$ mm^3).

We used the functional and structural T1-weighted images of all subjects as data input. The GM, WM, and CSF maps were spatially adjusted (sinc interpolation [or Whittaker–Shannon interpolation] of third degree) to the functional image, aiming to obtain functional segmented maps (GM, WM, and CSF). A multilinear regression was performed including WM and CSF global signal fluctuations and six movement parameters (three translational and three rotational) to reduce their confounding influence on the GM signal (101). Subsequently, a band-pass filter (0.008–0.1 Hz) was applied to remove low-frequency drifts and artifacts arising from cardiac or respiratory rate (102).

To reduce the chance of false positives/negatives, we controlled the amount of motion during scanning sessions using a cumulative value of movement equal or higher than 3 mm (size of one voxel) using the first volume as a reference as the cut-off to exclude subjects from the analysis. One patient was excluded from the resting-state analyses due to excessive movements during the fMRI acquisition. There was no difference between groups in the amount of movement during the scans: multivariate general linear model, Tukey's corrected with maximum displacement on axes X (controls average 0.77 mm ±0.47; patients average 0.78 ± 0.49), Y (controls average 0.30 mm ± 0.1; patients average 0.41 ± 0.22), and Z (controls average 1.15 mm ± 0.47; patients average 1.35 ± 0.51), average framewise displacement (controls average 0.18 mm ± 0.04; patients average 0.24 ± 0.06), and derivative variance (DVAR) (control average 3.18% *SD* ± 0.40; patients average 3.22% *SD* ± 0.36) were added as variables.

We estimated the cross-correlations using a cubic seed ($9 \times 9 \times 9$ mm^3) to extract the reference time-series (64). The reference time-series was correlated with each gray matter voxel creating the correlation maps. We varied the seed position according to the analysis described below.

DMN Analysis

The motivation to investigate the connectivity of the whole brain to and from the DMN came from the fact that: (a) it is a very stable and reproducible network (103, 104), (b) several studies have shown alterations in the DMN in ASD, including high functioning autism (88), and (c) it connects to most regions of the brain, and in particular, to regions processing salience, attention, and negative affect (105). To study the DMN, we positioned the seed on the PCC (centered on the MNI coordinate −41 13 −29) because this is one of the most active areas within the DMN, and it is possible to place a seed region involving both hemispheres at once (the blue square in **Figure 1** illustrates the position of this seed). We used the standard seed-based FC methodology, in which the whole averaged time series of the seed region is used as a reference to calculate the correlation with the GM voxels. We performed these steps individually generating a 3D r-score map for each volunteer. We converted all individual r-score maps resultant from the connectivity analysis to z-scores (Fisher's transformation) and performed a spatial smoothing ($6 \times 6 \times 6$ mm^3 FWHM), aiming to reduce high discrepancies in neighbor voxels.

Other Seed Positions

Additional to the seed positioned in the PCC (from the DMN), we tested other four seeds that we judged relevant for ASD verbal communication and social skills, according to findings from previous publications (6, 37, 106): (i) bilateral medial frontal region (MNI 0 49 −3); (ii) left + right amygdala (MNI −23 −4 −20); (iii) left anterior hippocampus (MNI −24 −13 −20); (iv) left temporal pole (−41 13 −29). We used the same steps as described for the generation of the 3D r-score *DMN* maps to obtain individual 3D statistical maps for the functional connectivity maps derived from seeds in these four positions. We did not include seeds in other areas also considered important for ASD, such as the caudate, to avoid too many comparisons

and to focus mainly on regions more directly related to emotional communication and interpersonal interactions.

The functional connectivity preprocessing was developed aiming to avoid possible confounding effects raised from structural variations. The functional images were segmented using the tissues probabilistic maps obtained from the T1WI, with consistent thresholds. This means that the resultant post-processed functional images included only voxels with the upper threshold probability to be GM or GM/WM. Additionally, the seeds time series extraction applied an algorithm that excludes by the average time series, voxels with a temporal behavior that is considered a minor outlier regarding the others. These last steps exclude from the seed, voxels which are functionally discrepant (see **Supplementary Image 1**).

As in the previous section, all individual r-score maps resultant from the connectivity analysis to z-scores (Fisher's transformation) and performed a spatial smoothing ($6 \times 6 \times 6$ mm^3 FWHM), aiming to reduce high discrepancies in neighbor voxels. We applied a two-sample *t*-test (to adjust for multiple comparisons we considered a $p < 0.001$, with a minimum of 10 contiguous voxels) with age added as covariate to compare controls and patient's groups resulting in two t-maps: a map showing areas that were more functionally connected in controls than in patients and a map showing the opposite.

Correlations With the Clinical Phenotype

We explored how the neuroanatomical and functional differences observed in the ASD group may be related to the clinical outcome. For that purpose, we conducted multiple correlation analyses between the ROI measures of cortical thickness, cortical area, and LGIs for the 33 gyral regions of each hemisphere generated by FreeSurfer (98, 99) and values from the PCC seed-based functional connectivity analysis (Resting-state analysis) vs. the "Current" Scores obtained at the ADI-R (scores in each of the three content areas: communication and language, social interaction, and restricted, repetitive behaviors), with age and total IQ as covariates and with Bonferroni correction for multiple comparisons using SPSS Statistics version 20 (IBM Corp. Released 2011. IBM SPSS Statistics for Windows, Version 20.0. Armonk, NY: IBM Corp.).

Analyses of Overlapping of Abnormalities Across Modalities

We analyzed the number of voxels that coincided with the resting-state fMRI and structural analyses using co-registration of statistical maps. This procedure was automated and based on the maps matrix intersection, providing relative percentages of overlapping among maps. Maps with distinct resolution were interpolated using 4th degree B-Spline interpolation.

In addition, we also investigated if the areas of abnormalities were near or within the same anatomical sub-region by sub-region by atlas labeling coincidence.

RESULTS

Subject Demographics and Global Brain Measures

There were no significant differences in age between ASD ($n = 22$; mean $\pm$ *SD*: 17.45 ± 3.29) and controls ($n = 29$; 18.48 ± 2.82, two-sample *t*-test, $p = 0.24$). There was no significant difference in sex ratios between groups (Fisher's exact test; $p = 0.22$). We found no significant differences in full scale and performance IQ ($p = 0.1$) but, as expected, the ASD group displayed significantly lower verbal scale IQ ($p = 0.03$; see **Table 1**). There were also no significant between-group differences in total brain volume or total surface area ($p > 0.05$).

All imaging analyses were covaried for age and total IQ and corrected for multiple comparisons as described in the methods.

Voxel-Based Morphometry (VBM) Analysis

VBM showed that individuals with ASD had reduced GM concentration in the cerebellum bilaterally (right anterior and posterior lobe and left posterior lobe), bilateral anterior cingulate, right middle, medial, and superior frontal gyrus, left fusiform gyrus, parahippocampus, amygdala, paracentral, and postcentral gyrus and claustrum. Increased GM concentration was detected in the right cerebellum and brainstem (**Figure 2**; **Table 2**).

In a correlation between age and GM volumes (i.e., areas with decreased GM volume in patients with increasing age as compared to controls), we observed that ASD participants had more age-related GM atrophy than controls exclusively in the left temporal lobe (temporal pole, middle temporal gyrus, parahippocampal gyrus, uncus) ($p < 0.001$, **Supplementary Image 2**; **Table 3**).

TABLE 1 | Summary of clinical data.

	Controls ($n = 29$)	ASD ($n = 22$)
Age	18.48 ± 2.82 SD	17.45 ± 3.29 SD
(range)	(14–25)	(14–25)
Sex	19M:10F	18M:4F
Handedness Rt to Lt	28:1	19:3
Full scale IQ	105.83 ± 9.64	99.77 ± 9.5
(range)	(90–127)	(87–121)
Performance IQ	107.79 ± 11.91	101.77 ± 12.25
(range)	(86–128)	(84–129)
Verbal IQ*	103.86 ± 9.53	98.95 ± 9.67
(range)	(87–123)	(85–124)
ADI-R social	–	20.50 ± 5.38
(range)		(10–29)
ADI-R communication	–	13.82 ± 4.36
(range)		(6–21)
ADI-R repetitive behavior	–	6.50 ± 1.78
(range)		(3–10)

*ADI-R, Autism Diagnostic Interview-Revised ("Current" Scores); ASD, autism spectrum disorder. There were no significant differences between the ASD and control groups in age, full IQ and performance IQ at $p < 0.05$ (two-tailed). There was no significant difference in sex ratios between groups (Fisher's exact test; $p = 0.22$). *There was a significant difference in verbal IQ ($p = 0.03$). The following cutoff scores were used: ADI-R social, greater than 10; communication, greater than 6; and repetitive behavior, greater than 3. Rt to Lt, right to left ratio.*

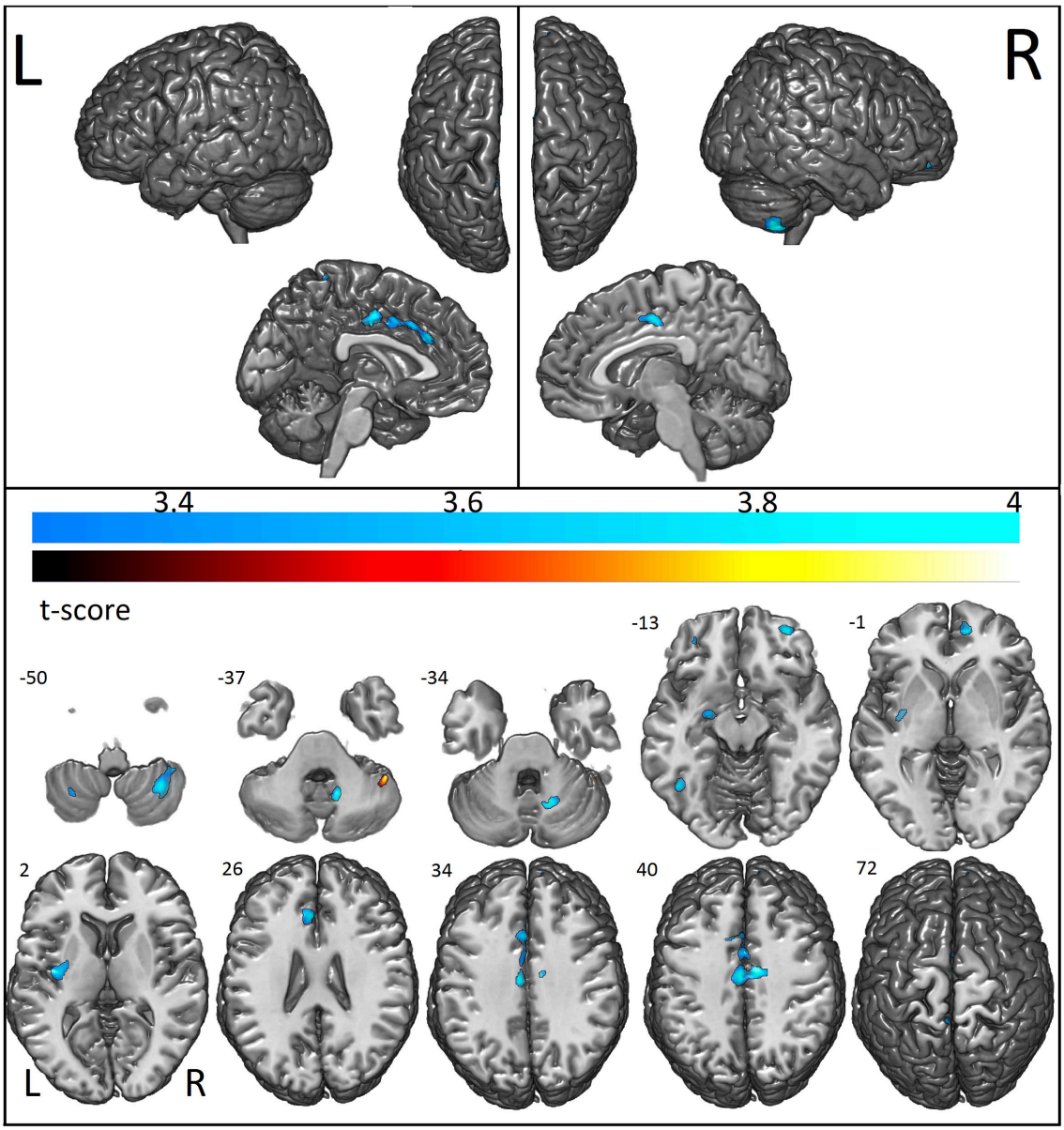

FIGURE 2 | Areas with decreased (cool colormap) and increased (hot colormap) cortical voxel-based morphometry in patients when compared to controls. In shades of blue (cool colormap), the most significant regions with decreased gray matter (voxel-based morphometry, two sample *t*-test, $p < 0.001$, cluster with at least 30 voxels) in patients compared to controls. In the hot colormap (black to yellow), regions of increased gray matter (voxel-based morphometry, two sample *t*-test $p < 0.001$ clusters with at least 30 voxels).

Cortical Thickness and Gyrification Index Using Freesurfer

Vertex-by-Vertex Analysis

Individuals with ASD presented decreased cortical thickness in the right hemisphere over the cingulate, precentral, superior frontal, superior, and inferior parietal regions. In the left hemisphere, decreased cortical thickness was observed in the supramarginal, superior parietal, paracentral, precuneus, superior, and middle frontal and lingual gyrus (the areas of decreased cortical thickness are shown in red in **Figure 3A**), and increased thickness was observed in the postcentral area (**Table 4**).

The ASD group had increased cortical surface in the following areas in the right hemisphere: cingulate, precentral, and superior frontal regions (which coincided with regions with decreased cortical thickness), as well as middle frontal, pars triangularis, supramarginal, precuneus, paracentral, superior, and middle temporal, and lateral occipital regions. In the left hemisphere, the ASD group had increased surface areas in the superior and middle frontal and precuneus (coinciding with the regions with

TABLE 2 | Areas of reduced gray matter concentration and increased gray matter concentration by VBM in patients with ASD in comparison with a group of healthy individuals.

Voxels	Area	Side	T score	MNI Coordinates
AREAS OF REDUCED GRAY MATTER vbm CONCENTRATION IN PATIENTS WITH ASD				
1804	Cerebellum, Posterior lobe	Right	4.24	33 −55 −53
259	Fusiform gyrus	Left	4.58	−44 −54 −8
347	Cerebellum, Anterior lobe	Right	4.45	14 −60 −30
1562	Cingulate gyrus	Left	4.43	−6 −13 37
	Cingulate gyrus	Right	4.25	8 −9 42
	Paracentral lobule	Left	4.25	−8 −9 45
263	Middle frontal gyrus	Right	4.42	32 53 −14
642	Claustrum	Left	4.12	−38 −10 3
170	Medial frontal gyrus	Right	4.06	12 51 1
66	Parahippocampal gyrus	Left	3.89	−15 −18 −26
121	Lentiform nucleus	Left	3.85	−18 −9 −9
	Amygdala	Left	3.74	−26 −7 −14
73	Postcentral gyrus	Left	3.72	−6 −42 70
77	Cerebellum, Posterior lobe	Left	3.69	−30 −58 −48
37	Superior frontal gyrus	Right	3.57	12 60 30
32	Cingulate gyrus	Right	3.49	18 33 22
AREAS OF INCREASED GRAY MATTER vbm CONCENTRATION IN PATIENTS WITH ASD				
96	Cerebellum, Posterior lobe	Right	3.93	45 −45 −38
42	Brainstem	Left/right	3.52	−2 −37 −27

TABLE 3 | Areas with significant gray matter VBM reduction influenced by the age in patients with ASD.

Voxels	Area	Side	T–score	MNI Coordinates		
378	Middle Temporal Gyrus	Left	3.98	−45	6	−36
112	Parahippocampal	Left	3.65	−21	−10.5	−34.5
78	Uncus/Amygdala	Left	3.88	−33	−10.5	−37.5
67	Superior Temporal Sulcus/Gyrus	Left	3.52	−63	−34.5	13.5

*$p < 0.001$; cluster with at least 30 voxels. All these four areas had significantly reduced functional connectivity on the seed analysis (see **Table 6**).*

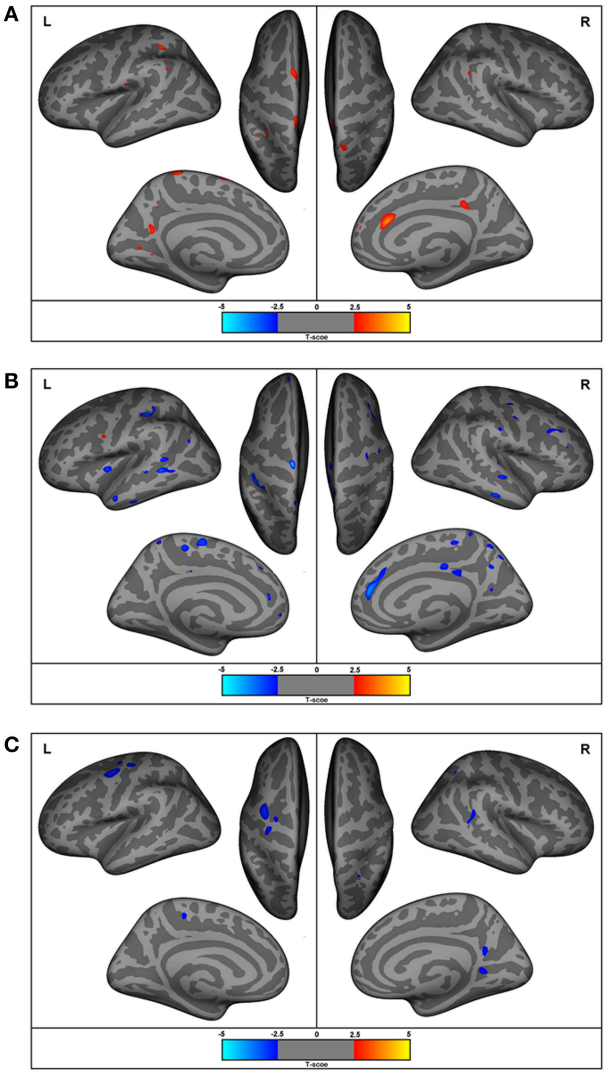

FIGURE 3 | Regions with differences in cortical thickness, surface areas, and gyrification. The most significant clusters for group analysis using a GLM vertex-wise approach, between control and autism groups for left and right hemispheres. In red are areas of decreased and in blue are areas of increased values in patients with autism. All results were corrected for multiple comparisons (Cluster-based correction). **(A)** ASD presented decreased (in red) cortical thickness in the right cingulate, precentral, superior frontal, superior, and inferior parietal regions. In the left hemisphere, decreased cortical thickness was observed in the supramarginal, superior parietal, paracentral, precuneus, superior, and middle frontal and lingual gyrus, and increased thickness in the postcentral area. **(B)** Increased surface areas in the superior and middle frontal and precuneus (coinciding with the regions with reduced cortical thickness), as well as in the pre- and post-central, orbitofrontal, posterior cingulate, inferior parietal, temporal lobe (superior, middle, inferior temporal), and insular regions in ASD. **(C)** Increased gyrification in the lingual, precuneus, superior temporal sulcus, and superior parietal areas in the right hemisphere and the precentral and paracentral areas of the left hemisphere.

reduced cortical thickness), as well as in the pre- and post-central, orbitofrontal, posterior cingulate, inferior parietal, temporal lobe (superior, middle, and inferior temporal regions) and insular regions (**Figure 3B**).

Gyrification was increased in the lingual, precuneus, superior temporal sulcus and superior parietal areas in the right hemisphere, and in the precentral and paracentral areas of the left hemisphere (**Figure 3C**).

Region of Interest (ROI) Analysis With FreeSurfer Data

When examining gyral-based differences in cortical thickness (ROI analysis with data extracted from FreeSurfer), which includes a larger number of voxels in each region measured by the vertex-by-vertex analysis, we observed increased thickness in the right posterior cingulate cortex, including the isthmus cingulate (which is a narrow cortical area that connects the posterior end of the cingulate gyrus with the parahippocampal gyrus), and in the right and left lateral orbitofrontal cortex as well as decreased cortical thickness in the left paracentral and posterior cingulate

TABLE 4 | Areas of decreased cortical thickness by FreeSurfer vertex-wise analysis in patients with ASD.

Cluster	*p*-value	X	Y	Z	Vertex	Anatomical region	Macro anatomical region
		MNI Coordinates					
LEFT HEMISPHERE							
1	0.001	−36.5	−43.67	9.21	58690	Inf. Supramarginal G	Supramarginal
2	<0.001	−21.47	−68.69	12.95	146808	Superior Temp S	Superior temporal sulcus
3	0.001	−13.68	−18.6	52.44	41967	Postcentral G	Postcentral
4	0.004	−0.05	−53.7	47.49	81380	Intraparietal S	Superior parietal
5	0.004	−13.64	−88.19	−5.07	101248	Middle occipital G	Occipital
6	0.001	8.59	11.93	64.19	44865	Sup. part of precentral S	Precentral
7	0.002	−23.88	−69.23	−38.08	69991	Inferior temporal S	Temporal
8	0.003	16.3	−65.67	53.17	53854	Superior parietal G	Superior parietal
9	0.001	28.43	−65.42	20.57	64736	Precuneus G	Precuneus
10	0.001	28.96	−12.24	53.54	26765	Sup. Frontal G	Paracentral
11	0.002	27.57	42.06	56.47	152760	Sup. Frontal G	Superior frontal
12	0.003	−6.05	96.89	−21.68	58366	Middle frontal G	Rostral middle frontal
RIGHT HEMISPHERE							
1	0.004	8.66	19.20	50.53	29786	Sup. part of precentral S	Precentral
2	0.003	20.9	72.25	−1.21	4081	Sup. frontal G	Superior frontal
3	0.002	−10.97	7.58	66.56	5767	Precentral G	Precentral
4	0.005	−9.49	89.20	−46.04	119767	Orbital G	Pars orbitalis
5	<0.001	−30.83	17.08	42.62	108535	Postcentral G	Postcentral
6	0.001	−26.24	−73.11	12.69	45913	Sup. temporal S	Superior Temporal sulcus
7	0.001	−26.08	28.49	63.48	144822	Central S	Precentral

Level of significance equal to 0.01. All results were corrected for multiple comparisons (cluster-based correction). S, sulcus; G, gyrus.

and in the right temporal pole in the ASD group compared to controls (**Supplementary Image 3**; **Table 5**).

The ROI analysis showed significantly increased cortical surface area only in the right anterior cingulate ($p = 0.019$, multivariate analysis with Bonferroni correction).

We found also increased gyrification index in the postcentral, precentral, superior parietal, and supramarginal regions of both hemispheres, in the right frontopolar and middle frontal regions, and in the left paracentral region (**Table 6**).

Subcortical Volumes

We found no differences between groups in the volumes of the amygdala, hippocampus, thalamus, or caudate.

Functional Connectivity

We first examined the FC patterns of the PCC, which is part of the DMN. Relative to the control group, ASD patients showed reduced FC with the PCC (i.e., between the posterior part of the DMN and other areas of the brain) which was more pronounced in the left hemisphere, including the middle temporal gyrus, inferior, and superior frontal gyrus, and anterior and posterior cingulate. Decreased connectivity was also observed in other regions outside the DMN: the right cerebellum, cuneus, and caudate (**Figure 4**). Increased FC in areas of the DMN occurred only in the right middle frontal gyrus. Outside the DMN regions, increased connectivity was present in the left caudate (**Figure 4**).

The analysis of the additional seed positions as described in Methods, showed decreased FC in ASD patients between the left amygdala and right claustrum, inferior parietal lobule, postcentral gyrus, cingulate gyrus, precentral gyrus, inferior frontal gyrus, middle frontal gyrus, and left postcentral gyrus; between the left anterior frontal region and the right superior frontal gyrus; between the left anterior hippocampus and bilateral temporal, right insula, and left precentral regions; between the left temporal pole and the left temporal and parietal, right temporal, frontal, parietal, and occipital regions (**Figure 4**; **Table 7**). Increased FC was observed between left amygdala and right superior frontal gyrus, and between the middle frontal regions and bilateral pre- and postcentral gyrus (**Figure 4**; **Table 7**).

Imaging and Clinical Scores

Cortical Thickness and Symptomatology

Significant correlation (corrected for age and total IQ) was found in the right pars triangularis (part of the lateralized fronto-parietal components of the DMN) (73), where reduced cortical thickness was associated with more impaired scores in the social domain of the Autism Diagnostic Interview-Revised (ADI-R) ($r = -0.63$; $p < 0.001$) (**Figure 5**). A significant negative correlation ($r = -0.52$; $p = 0.02$) was also found between cortical thickness in the left precentral and superior frontal regions (areas of the executive control and sensorimotor component of the DMN) (73) with communication scores on the ADI-R (**Figure 6**).

TABLE 5 | Spatially distributed patterns of differences in cortical thickness in individuals with Autism spectrum disorder compared with controls—ROI analysis.

Lobe	Region	Side	Centroid MNI coordinates		
			x	y	z
		ASD>Controls			
Frontal	Lateral orbito-frontal	L	28.96	−12.24	53.54
	Lateral orbito-frontal	R	21	38	−19
Limbic	Posterior cingulate cortex/Isthmus cingulate	R	9	−39	14
		ASD<Controls			
Temporal	Temporal pole	R	42	21	−35
Limbic	Posterior cingulate	L	−7	−41	30
Other	Paracentral	L	−8	−32	69

L, left; R, right. $p < 0.05$ (multivariate analysis with Bonferroni correction) for all the areas presented in the table.

TABLE 6 | Spatially distributed patterns of differences in the gyrification index in individuals with Autism Spectrum Disorder compared with controls—ROI analysis.

Lobe	Region	Side	Centroid MNI coordinates		
			x	y	z
		ASD>Controls			
Frontal	Frontopolar	R	21	29	−23
	Middle frontal	R	63	8	37
Parietal	Superior parietal	L	−28.43	−65.42	20.57
	Superior parietal	R	28	−63	52
	Supramarginal	L	−36.5	−43.67	9.21
	Supramarginal	R	42	−38	32
	Paracentral	L	−8	−32	69
Central	Postcentral	L	−13.68	−18.60	52.44
	Postcentral	R	−30.83	17.08	42.62
	Precentral	L	8.59	11.93	64.19
	Precentral	R	−10.97	7.58	66.56

L, left; R, right. $p<0.05$ (multivariate analysis with Bonferroni correction) for all the areas presented in the table.

Reduced cortical thickness in these areas was associated with more severe scores on the ADI-R communication domain. Thicker cortices in the right temporal pole ($r = 0.56$; $p = 0.01$) and posterior cingulate ($r = 0.50$; $p = 0.03$) were associated with greater communication impairment as measured by the ADI-R communication domain (**Figure 6**). We found no correlations between the scores on the restrictive and repetitive behaviors (RRIB) domain of ADI-R and structural images.

Functional Connectivity and Symptomatology

There was a trend for significant association (that did not survive Bonferroni correction) between stronger connectivity indexes from PCC to the right temporal pole ($p = 0.09$) and left anterior hippocampus ($p = 0.10$) with worse symptom severity in the social domain on the ADI-R, controlling for age and total IQ. We found no correlations between the scores on the RRIB domain of ADI-R and FC.

Overlap of Abnormalities Across Modalities

The percentage of coincident maximum voxels abnormalities between resting-state FC and abnormal gray matter on VBM was <3%. However, we found a close localization of the FC abnormalities and GM reduction on VBM and changes in cortical thickness in FreeSurfer ROI analysis (**Figure 7**) and vertex-wise analysis (**Figure 8**) in cingulate gyri of both hemispheres, left parahippocampal gyrus, postcentral gyrus, amygdala, and claustrum; right middle and superior frontal gyri, temporal pole, and cerebellum (**Table 8**).

Note that the lack of correspondence between the maps presented in **Figures 2**, **3** and the results in **Figures 7**, **8**, is because in **Figures 2**, **3** the maps show the most statistically significant clusters of abnormalities while in **Figures 7**, **8** the areas indicated do not correspond to the maximum voxel statistical location, but rather the sub-anatomical regions with significant differences (therefore, much larger than in **Figures 2**, **3**).

GM atrophy determined by VBM showed a closer anatomical relationship with reduced FC than surface measures by FreeSurfer. Interestingly, areas with decreased GM volume (middle and superior temporal gyri, parahippocampus, and amygdala/uncus, all in the left hemisphere) that correlated with increasing age in patients had reduced FC (see **Table 3**).

DISCUSSION

The diversity of neuroimaging results are likely explained by the heterogeneous nature of ASD, both among the subgroups within the spectrum, the variable comorbidities and on an individual level across the lifespan (15, 29, 35, 43, 44, 50, 57–60, 63, 67, 84–86, 107, 135). The individual differences in functional and structural organization, the idiosyncratic ASD connectivity and cortical atrophy maps, which change over the maturation of central nervous system, are themselves the core features of ASD, although its pathophysiological basis remains undetermined (13, 15). These findings underscore the need to address both age and severity when investigating functional and structural neuroimaging in ASD (15). Every imaging technique, both regarding acquisition and post-processing have their limitations and advantages and are in constant improvement of the quality of acquisition (better hardware) and algorithms of post-processing. These facts make it difficult to compare studies over the years. The use of multimodal imaging in a single study, in a similar age range and severity of symptoms, may provide a better description of the altered brain connectivity and structural changes, and its relationship with behavioral changes, than one imaging method alone. However, several multimodal studies have been performed with some contradictory findings, which by itself justify further studies (6, 15, 29, 35, 37, 43, 44, 50, 57–60, 63, 67, 84–86, 107, 135).

Different from most studies that focused on a single technique (27, 28, 108–112) or low functioning autism (113), or using a heterogeneous group of patients (114), our multimodal imaging

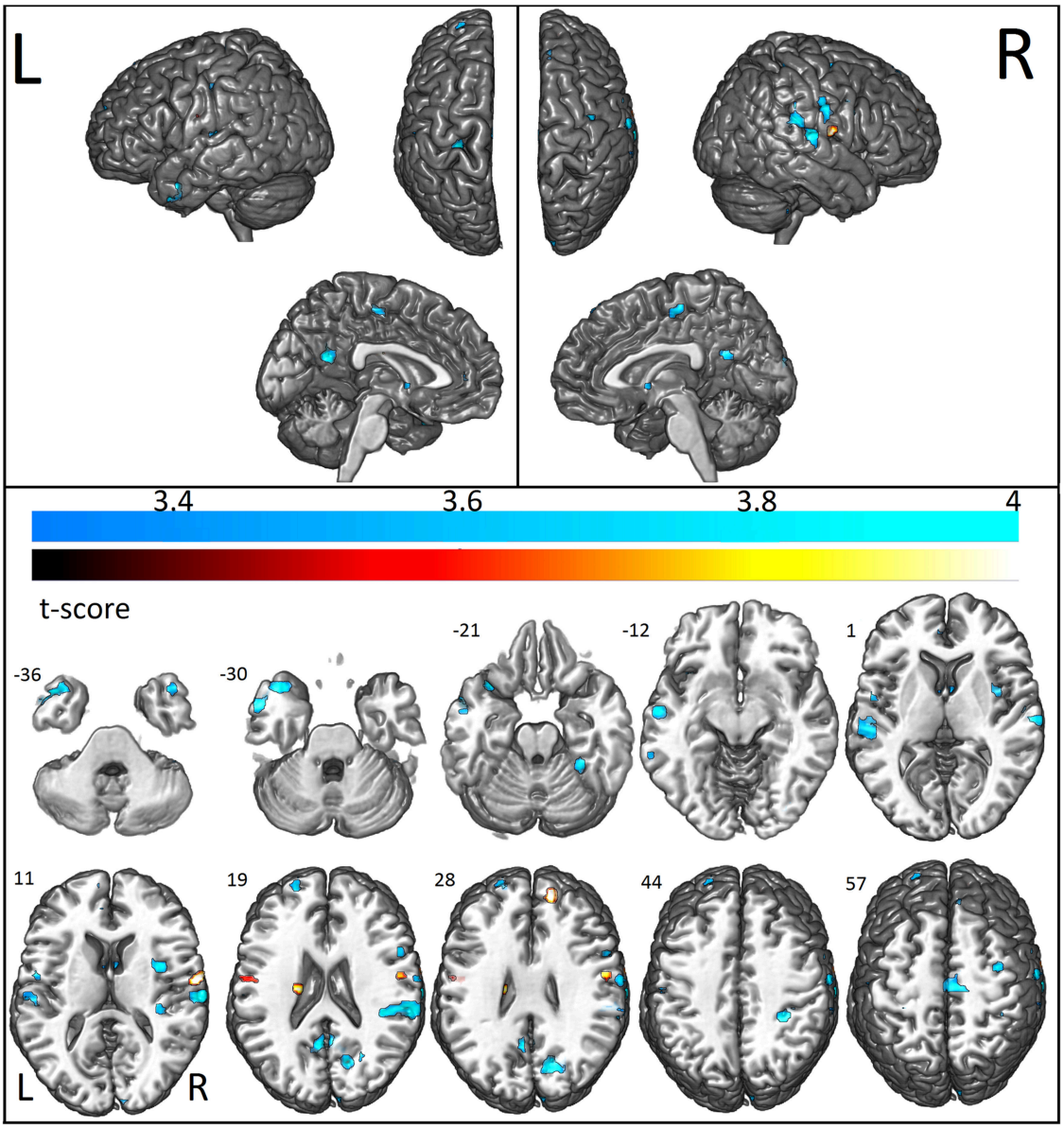

FIGURE 4 | Areas with decreased (cool colormap) and increased (hot colormap) functional connectivity measurements in patients when compared to controls. In shades of blue (cool colormap), regions with maximum decreased functional connectivity (union of all seeds results, two sample *t*-test $p < 0.001$ clusters with at least 10 voxels) in patients compared to controls. In the hot colormap (black to yellow), regions of increased functional connectivity (two sample *t*-test, $p < 0.001$, cluster with at least 10 voxels).

investigation showed abnormalities across brain measures in young adults and adolescents with high-functioning autism. We showed reduced cortical thickness, increased cortical surface and increased gyrification, as well as abnormal functional connectivity, mostly co-localized in areas that are important hubs of the default mode network and other regions frequently linked to socio-emotional processing, such as cingulum, amygdala, insula, and temporal pole. Overall, our findings suggest aberrant functional connectivity involving a network of altered cortical structure.

We combined structural and functional connectivity analyses to detect complex brain abnormalities and to investigate how these alterations are related to each other and symptom severity in a group of individuals with high functioning autism. We observed that patients with ASD had decreased FC compared to controls between the PCC and anterior medial prefrontal cortex and left superior temporal cortex (temporal pole), both regions part of the DMN. Patients also exhibited greater diffuse subtle GM atrophy related to increasing age (in the VBM analysis), more pronounced in left temporal

TABLE 7 | Areas of significantly decreased and increased connectivity in patients with ASD in comparison with a group of healthy individuals.

Seed region	Voxels	Area	Side	T score	MNI Coordinates
AREAS OF DECREASED FUNCTIONAL CONNECTIVITY IN PATIENTS WITH ASD					
PCC*	47	Middle temporal gyrus	Left	4.66	−54 5 −26
PCC	56	Cuneus	Right	4.64	15 −70 25
PCC	83	Inferior frontal gyrus	Left	4.49	−39 17 −26
PCC	35	Posterior cingulate	Left	4.25	−6 −55 28
PCC	33	Superior frontal gyrus	Left	4.01	−21 59 25
PCC	20	Caudate	Right	3.82	3 2 −2
PCC	14	Cerebellum, Posterior lobe	Right	3.70	45 −37 −44
PCC	12	Anterior cingulate	Left	3.50	−6 44 13
Left amygdala	44	Insula	Right	4.47	36 2 13
Left amygdala		Claustrum	Right	3.57	27 8 19
Left amygdala	172	Inferior parietal lobule	Right	4.30	53 −31 22
Left amygdala		Postcentral gyrus	Right	3.83	53 −19 13
Left amygdala	44	Cingulate gyrus	Right	4.20	30 −34 40
Left amygdala	33	Precentral gyrus	Right	4.08	36 −4 55
Left amygdala	21	Inferior frontal gyrus	Right	3.89	54 11 25
Left Amygdala	44	Middle frontal gyrus	Right	3.88	3 −16 52
Left Amygdala	12	Postcentral gyrus	Left	3.44	−57 −15 43
Left ant. frontal	15	Superior frontal gyrus	Right	3.61	9 41 55
Left ant. hippocampus	84	Superior temporal gyrus	Left	4.20	−54 −28 4
Left ant. hippocampus		Transverse temporal gyrus	Left	4.03	−54 −19 10
Left ant. hippocampus	54	Superior temporal gyrus	Right	4.08	66 −19 10
Anterior hippocampus	33	Insula	Right	3.92	36 −28 13
Left ant. hippocampus	12	Precentral gyrus	Left	3.66	−54 −1 10
Left ant. hippocampus	10	Inferior frontal gyrus	Right	3.51	66 14 28
Left temporal pole	50	Postcentral gyrus	Left	4.31	−27 −28 67
Left temporal pole		Inferior parietal lobule	Left	3.45	−30 −34 58
Left temporal pole	34	Middle temporal gyrus	Left	4.25	−57 −10 −11
Left temporal pole	34	Cerebellum, Anterior lobe	Right	4.25	30 −40 −20
Left temporal pole		Parahippocampal gyrus	Right	3.49	27 −25 −20
Left temporal pole	28	Medial frontal gyrus	Right	4.25	12 −19 58
Left temporal pole	47	Superior temporal gyrus	Left	4.14	−48 8 −32
Left temporal pole	68	Postcentral gyrus	Right	4.00	63 −10 31
Left temporal pole	22	Superior temporal gyrus	Right	3.84	42 17 −38
Left temporal pole	72	Posterior cingulate	Right	3.83	3 −52 22
Left temporal pole	28	Cuneus	Right	3.83	21 −76 28
Left temporal pole		Precuneus	Right	3.57	24 −67 25
Left temporal pole	20	Middle frontal gyrus	Right	3.74	63 8 37
Left temporal pole	11	Postcentral gyrus	Left	3.69	−54 −4 13
AREAS OF SIGNIFICANTLY INCREASED FUNCTIONAL CONNECTIVITY IN PATIENTS WITH ASD					
PCC	22	Caudate	Left	4.13	−18 −16 25
PCC	10	Middle frontal gyrus	Right	3.60	45 8 61
Left amygdala	28	Superior frontal gyrus	Right	4.78	15 53 28
Bil. medial frontal region	74	Postcentral gyrus	Right	4.04	63 −7 13
Bil. medial frontal region		Precentral gyrus	Right	3.51	54 −4 31
Bil. medial frontal region	32	Precentral gyrus	Left	3.40	−51 −10 25
Bil. medial frontal region		Postcentral Gyrus	Left	3.29	−60 −7 22

**PCC, Posterior Cingulate Cortex bilaterally (posterior aspect of the DMN). Ant, anterior; Bil, Bilateral; All regions in the table had $p < 0.001$ (two-sample t-test), cluster with at least 10 voxels.*

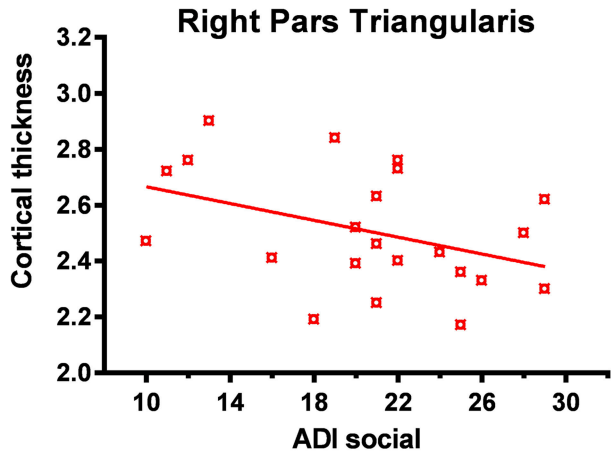

FIGURE 5 | Reduced cortical thickness (from FreeSurfer ROI analysis) in the right inferior frontal lobe correlated with higher social impairment. In the ASD group reduced cortical thickness in the right pars triangularis was associated with greater social impairment as measured by the ADI-R (Autism Diagnostic Interview-Revised) social domain.

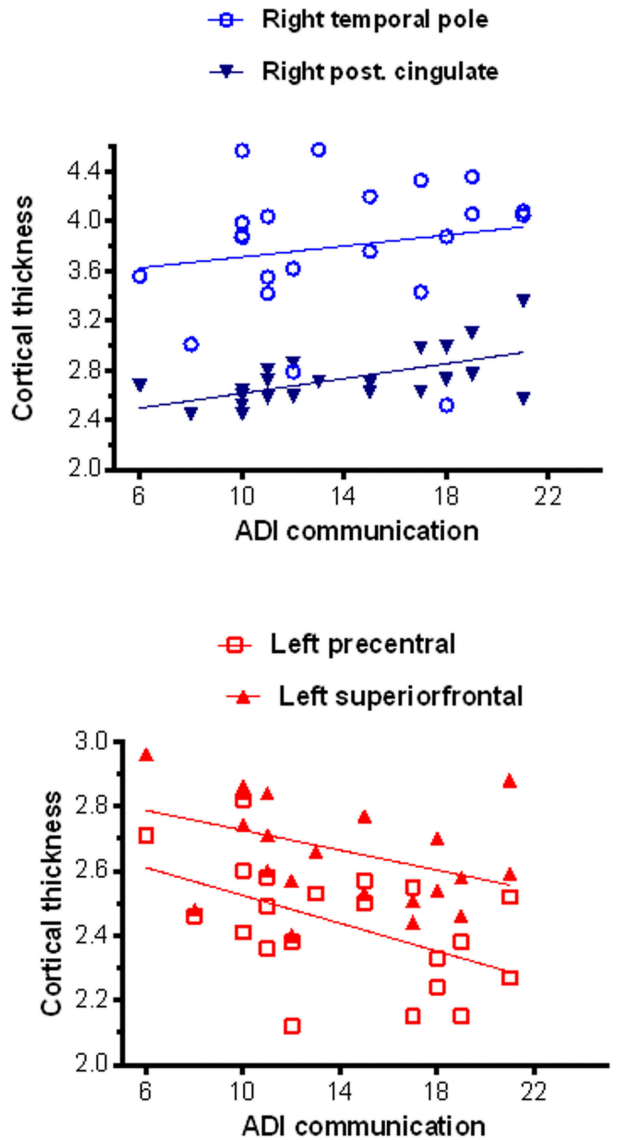

FIGURE 6 | Correlations between cortical thickness (from FreeSurfer ROI analysis) and communication scores on the ADI-R. In the ASD group thicker cortices in the right temporal pole and right posterior cingulated were positively associated with greater communication impairment as measured by the ADI-R Autism Diagnostic Interview-Revised) social domain **(Top)**, while thinner cortices in the left precentral and superior frontal regions correlated with greater communication impairment as in the ADI-R social domain **(Bottom)**.

regions (temporal pole, middle temporal gyrus, parahippocampal gyrus, and uncus). In addition, we showed areas of abnormal cortical structure, combining thinning, and thickening, increased surface area and gyrification index in different areas of the brain, involving frontal, parietal, and temporal areas that had abnormal FC. Overall these structural and functional abnormalities involved areas linked to: (a) visual processing and analysis of logical order of events (lingual gyrus), (b) encoding visual memories (temporal and posterior cingulate areas), (c) areas related to language, memory and emotion processing (temporal pole, middle temporal, parahippocampus, and uncus), (d) areas of the executive control component of the DMN, which has been associated with performance of executive functional tasks (anterior and posterior cingulate cortex, left middle temporal, inferior, and superior frontal gyrus), (e) areas of the sensorimotor component of the DMN (anteromedial prefrontal cortex and bilateral pre- and postcentral gyrus), (f) areas of the lateralized fronto-parietal components of the DMN related to executive and language functions (reduced cortical thickness in left frontal regions), and (g) areas of the auditory component of the DMN (temporal and parietal areas) (73, 115). In addition, more severe scores on the communication domain of the ADI-R were associated with increased cortical thickness in the right temporal and posterior cingulate gyrus, and there was a trend for worse symptoms in the social domain of the ADI-R to be associated with stronger connectivity between posterior cingulate cortices (DMN) and temporal regions (areas of the Auditory component of the DMN) (71–73).

Our findings taken together indicate that young adults and adolescents with high functioning autism present complex, subtle morphological cortical changes that may reflect different stages of neurogenesis, combined with aberrant connectivity within and outside the DMN.

Structural Abnormalities

To date, neuroimaging studies in ASD have mainly investigated either cortical volume or cortical thickness in isolation, and combined measures of surface area and gyrification with functional data remain scarce (4). Studies in adults with ASD typically show cortical thickening of the frontal cortex (6, 116, 117), whereas the cortical thickness of the temporal lobe has been reported as increased or decreased in patients with ASD (118).

Abnormal brain structure has been reported with great variability in individuals with ASD, both enlargement, and

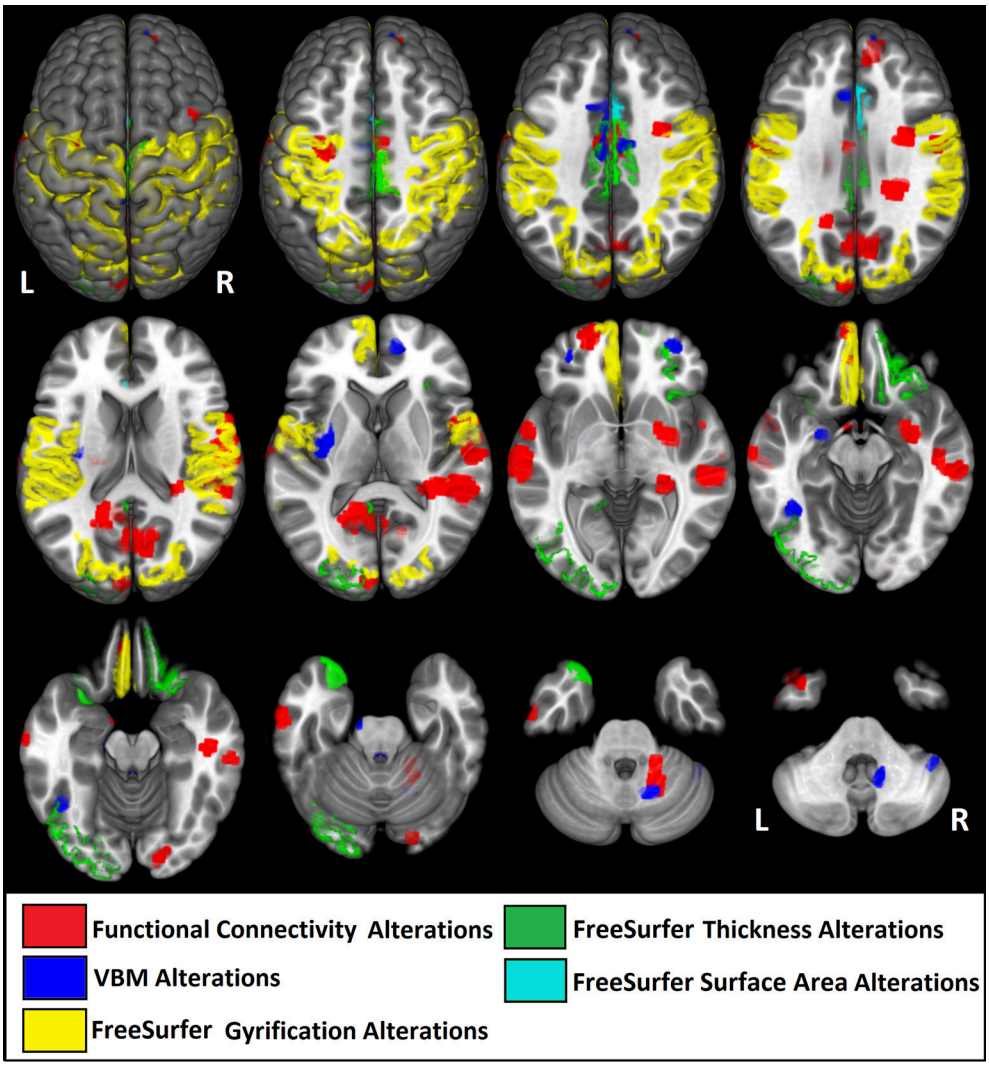

FIGURE 7 | Illustrative figure showing anatomical localization of abnormalities in functional connectivity (in red), voxel-based morphometry (VBM, in blue), and FreeSurfer ROI analysis of gyrification index (in yellow), cortical thickness (in green), and surface area (in light blue). The areas indicated in this figure do not correspond to the maximum voxel statistical location, but rather the sub anatomical regions with significant differences in patients with high functioning autism compared to controls. See **Tables 2**–**7** for the centroid MNI coordinates of maximal abnormalities and **Table 8** for a summary of the location of increased and decreased changes as compared to controls.

reduction of the GM (40, 46, 119). However, this variability is probably due to the highly heterogeneous age of the patients (from children to adults) and various phenotypes (5, 120). It is believed that in ASD there is a disruption of the time course of brain development and this could be the explanation for the detection of specific increased areas in children during an early phase of development and reduced areas (atrophy) in adults (40). Our findings, which included only ASD individuals with total IQ > 85, confirm this theory and add further evidence about specific types of abnormal cortical shape and volume in association to functional abnormalities. Another key aspect of our results is that we used multimodal imaging measures in the same patients to certify that the abnormalities are present across brain measures, different from most studies so far that focused on a single technique.

Volumetric studies of ASD in earlier MRI studies showed increased volumes in left frontal and temporal lobes across the 2- to the 11-year-age range (121) and in the dorsolateral prefrontal and medial frontal cortex in patients aged 2–5 years (122). A meta-analysis showed that brain size in autism was slightly reduced at birth, increased within the first year of life, and within normal range by adulthood (123). However, it is difficult to compare these studies since the methodologies for cortical volume measurements varied significantly (manual volumetry, VBM with different versions of SPM software, cortical thickness). Also, earlier studies used images with lower MRI field strength (1.5 T) as compared to the higher fields (3T MRI)

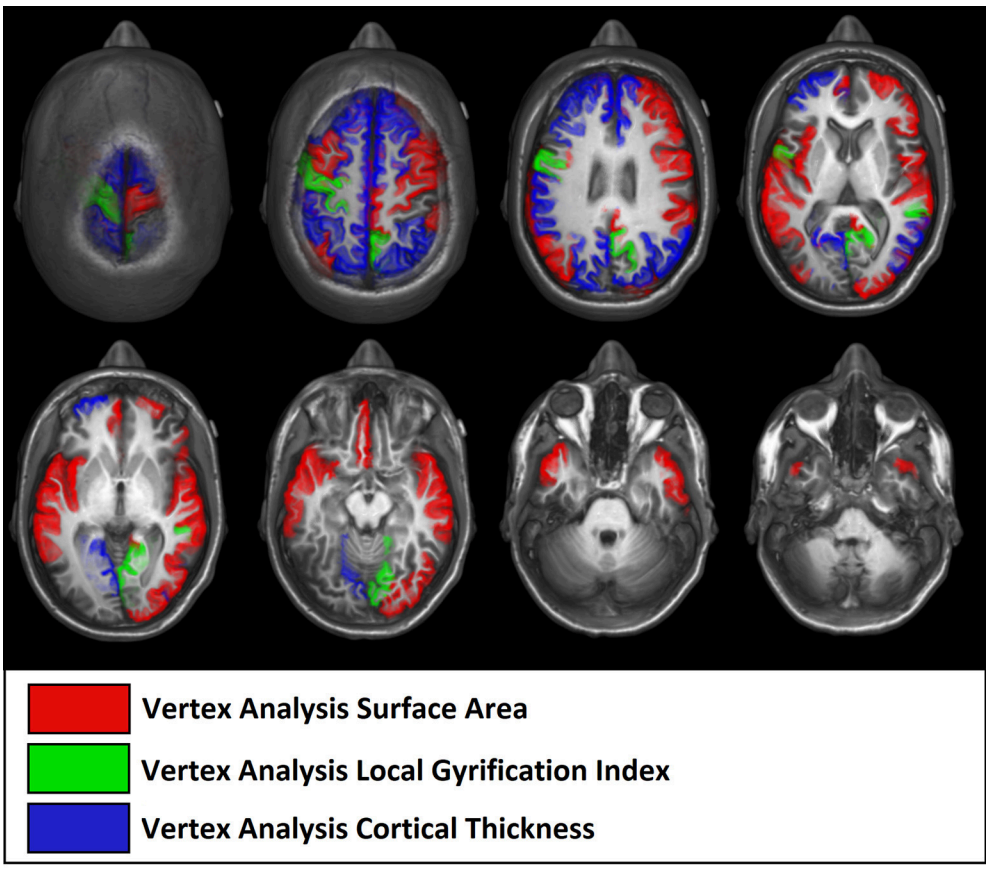

FIGURE 8 | Illustrative figure showing anatomical localization of abnormalities of FreeSurfer vertex-wise analyses of surface area (in red), gyrification index (in green), and cortical thickness (in blue). The areas indicated in this figure do not correspond to the maximum voxel statistical location, but rather the sub anatomical regions with significant differences in patients with high functioning autism compared to controls. See **Figure 3** and **Table 4** for the location of maximal abnormalities and **Table 8** for a summary of the location of increased and decreased changes as compared to controls.

and higher resolution images used in more recent studies. More recent versions of SPM software (http://www.fil.ion.ucl.ac.uk/spm/software/) have substantial algorithmic enhancements with more sophisticated registration models compared to previous versions and thus, making it difficult to compare earlier studies with more recent ones (45, 124). These aspects and the fact that our patient's ages ranged from 14 to 25 years (mean: 17.4 years) may explain why our VBM analyses (excluding the cerebellum and brainstem) did not show areas of increase GM and showed GM atrophy mainly in temporal and frontal areas.

VBM and FreeSurfer cortical measures use quite different methods and are expected to yield different results as we showed here. Our intention was not to compare these two methods, but rather to expand the search for structural changes in these patients in a multimodal way. We believe that these two techniques added information and were not redundant. VBM performs voxel-wise statistical analysis on smoothed (modulated) normalized segments (90, 124). VBM is a statistical parametric mapping of segmented tissue density and compares the local concentration of gray matter between two groups of subjects (90, 124). The interpretation of gray matter concentration or density depends on the preprocessing steps used (90, 124). However, VBM is a whole-brain unbiased, objective technique, with very reproducible results in similar circumstances (of image quality and software version), providing great sensitivity for localizing small-scale, regional differences in gray matter concentration (90, 124, 125). In addition, more rigorous methods for correction for multiple comparisons will reduce the false positives but also reduce the pickup rate of true positives.

FreeSurfer uses the cortical geometry to do inter-subject registration, which appears to have a much better matching of homologous cortical regions than other volumetric techniques. FreeSurfer allows measuring the two components of volume separately (thickness and surface area). These two measures are not similar and do not necessarily change in parallel as will be discussed below (37). FreeSurfer uses the white matter surface geometry for registration, which is completely independent to GM atrophy; therefore, GM alterations will not result in different registrations (92–94, 99). Therefore, one should not expect a total overlap between findings with VBM and FreeSurfer in the same group of subjects, as it was in this study.

TABLE 8 | Sub-regional overlap of abnormalities across structural and functional MRI modalities.

Lobe/Region	Area	GM/VBM		Cortical Thickness				Cortical Surf. area				Gyrification Index				FC of DMN	
				FS-VxV		FS-ROI		FS-VxV		FS-ROI		FS-VxV		FS- ROI			
		Left	R	Left	R	Left	R	Left	R	Left	R	Left	R	Left	R	Left	R
Frontal	Orbito-Frontal					↑	↑	↑									
	Cingulate	↓	↓		↓	↓	↑	↑	↑		↑					↓ ↑	↓
	Sup. Frontal		↓	↓	↓			↑	↑							↓	↓ ↑
	Middle Frontal		↓	↓				↑	↑						↑		↓ ↑
	Inf. Frontal/Pars triang.								↑							↓	↓
	Frontopolar														↑		
Temporal	Pole	↓				↓										↓	
	Sup. Temp. sulcus/G.	↓		↓			↓	↑								↓	↓
	Middle Temp. G.	↓			↓			↑	↑				↑			↓	↓
	Inf. Temp. G							↑	↑								
	Fusiform G	↓															
	Parahippocampus	↓														↓	
	Amygdala	↓														↓	↓
	Hippocampus															↓	
	Insula							↑									↓
	Claustrum	↓															
	Caudate															↑	↓
Central	Paracentral	↓		↓		↓	↓		↑			↑		↑			
	Precentral			↓	↓			↑	↑			↑		↑	↑	↓ ↑	↓ ↑
	Postcentral	↓		↓ ↑	↓			↑						↑	↑	↓ ↑	↓ ↑
Parietal	Supramarginal			↓					↑					↑	↑		
	Sup. parietal			↓	↓								↑	↑	↑		
	Inf. Parietal			↓	↓			↑								↓	↓
	Precuneus			↓				↑	↑				↑				
Occipital	Lingual G.			↓									↑				
	Lateral Occip.								↑								
	Cuneus																↓
Cerebellum	↓	↓ ↑														↓	↓

↓, Decreased ↑, increased. GM, gray matter; VBM, voxel-based morphometry; FS-VxV, FreeSurfer voxel by voxel analyses; FS-ROI, FreeSurfer voxel region of interest (ROI) analyses; FC, functional connectivity; DMN, default mode network, G, gyrus.

Using FreeSurfer, we found significant differences in cortical thickness of ASD patients over frontal regions (superior, middle frontal regions, pars orbitalis) and temporal lobes (right temporal pole). This finding is consistent with previous reports suggesting that people with ASD have differences in frontal lobe neuronal integrity, function, anatomy, and connectivity. Furthermore, it has been suggested that individuals with ASD have a delay in frontal lobe maturation and that abnormalities in frontal lobe development may underlie some of the social impairments reported in people with ASD (39, 122, 126), which was corroborated by our results.

Cortical surface areas are usually, but not necessarily, increased (as illustrated in **Table 7**) in regions with reduced cortical thickness, which is biologically explained by the consequent increase in sulcation of the cortical mantle (i.e., with atrophy the sulci became deeper, thus increasing the area) (37). Therefore, explaining our finding of increased cortical surface areas coinciding with the regions with reduced cortical thickness described above, as well as in the pre- and post-central, orbitofrontal, posterior cingulate, inferior parietal, temporal lobes, and insular regions. However, cortical thickness and surface area measurements represent distinct aspects of the cortical architecture and may represent different early neurodevelopmental pathologies (37, 127, 128). Cortical thickness measurements appear to reflect the number of neurons within cortical minicolumns (mainly related to intermediate progenitor cells), while cortical surface area measurements may be related to the number of cortical minicolumns (mainly related to radial unit progenitor cells), according to the radial unit hypothesis (5, 37, 117, 127–129). Our findings suggest that, in addition to the well-documented early brain overgrowth in ASD, there is probably an arrested growth during late childhood, followed by accelerated regionally specific thinning during adolescence and young adulthood. More specifically, the present results complement earlier findings of thinner cortices in adults with ASD (5, 130–132).

We found increased gyrification in temporal, parietal, and frontal areas in ASD, supporting previous studies that indicate that these are the core areas in ASD and are probably related to abnormalities in visual-spatial attention, selective attention, and visual-motor learning as well as in the mirror neuron system (133, 134). Gyrification represents the amount of cortex within sulcal folds in the surrounding area of measurement and is computed as the ratio between the surface of the outer surface of the brain and the surface of the corresponding area on the GM (pial) surface (37, 95, 129), which reflects an early developing process. It is believed that the brain in ASD goes through a stage of accelerated expansion during early childhood, and consequently, ASD patients are expected to have an increase in cortical folding to accommodate an increasing brain surface into the skull (37, 127). A closer inspection of **Figure 3**, reveals that the areas (representing the points of maximal statistical scores) of reduced cortical thickness, increased cortical surface areas and increased gyrification areas have a similar distribution in our group of young adults and adolescents with ASD.

Abnormalities found in our analysis could be implicated in the core behaviors often impaired in ASD: social and communication (medial frontal region, anterior cingulate) and repetitive and stereotyped behavior (medial and lateral orbitofrontal region).

Resting-State Functional Connectivity

Findings from most studies have continued to support the broad notion that, overall, individuals with ASD have poorer connectivity in regions spanning long distances in the brain compared to controls, whereas connectivity seems to be increased in local circuits (6, 47). However, findings amongst studies on FC in ASD do not overlap [some with increased (106) and others with decreased (51, 86, 135) connectivity in similar areas], in part due to different techniques used (i.e., seed analyses of predetermined areas, region of interest analyses, etc.) and heterogeneity of patient groups and age range, as occurs with the structural data discussed above (53, 68, 107). Others have reported decreased connectivity of the DMN in adolescents and adult patients with ASD (14, 51, 52, 54, 87), associated with more severe symptoms (135, 136). We found increased connectivity in the ASD group in the right middle frontal gyrus, and a trend for an association between the right temporal pole and left anterior hippocampus FC strength and ADI-R social score, indicating that worse symptom severity was associated with more connectivity in this region. Overall, our results are similar to those observed by Supekar et al. (106) about brain hyperconnectivity predicting symptom severity in ASD. Individuals with greater FC showed more severe social deficits, and they argue that this brain-behavior relationship suggests that aberrant FC may underlie social deficits, which are some of the hallmarks of ASD (28, 106). Our results add to the growing evidence that regional DMN under-connectivity may underlie the pathogenesis of patients' clinical deficits and go further by showing that seed-based analysis reveals the reduction in connectivity also in areas outside the DMN (amygdala, insula, and temporal pole), supporting that ASD is not only a condition of under- or hyper-connectivity but also of aberrant FC (13, 14, 27, 29, 35, 37, 54–56, 69, 137–140).

The Role of the Temporal Pole

We found significant VBM cortical atrophy in ASD individuals when considering age, only in the left temporal lobe, including the left temporal pole. We also observed decreased FC in individuals with ASD between the left temporal pole and the remainder of left temporal and parietal regions. This region lies between the orbital frontal cortex and the amygdala, two of the region's most frequently linked to socio-emotional processing. The temporal pole is highly connected with the amygdala, hippocampus, parahippocampal gyrus, cingulate gyrus, orbitofrontal cortex, and the insula (141, 142). In addition, the temporal pole cortex extends topographically to the insula (ventrally) and the entorhinal cortex (medial-inferiorly) (142). The role of the temporal pole is key for various social and emotional functions, including mentalizing (theory of mind) (56, 66, 141, 143, 144). The impairment of theory of mind abilities is one of the most popular hypotheses about ASD (56, 66, 86, 144–146). Some studies using theory of mind tasks showed

temporal pole activation (147–150), which give support to our interpretation of the temporal pole as a key node in ASD and social dysfunctions.

Overlap Between Functional and Structural Findings

Our findings give further evidence that ASD is a network disorder, as revealed by the structural and functional abnormalities (112, 151). In a similar vein, Honey et al. observed that, although resting-state FC is variable and is often present between regions without direct structural linkage, its strength, persistence, and spatial statistics are nevertheless constrained by the large-scale anatomical structure of the human cerebral cortex (152).

We found no complete voxel overlap of areas of maximal GM reduction and areas of decreased connectivity in our patients, which is expected due to the different anatomical resolution between structural and functional images (original voxel sizes of 1 vs. 3 mm^3, which became even more discrepant after spatial smoothing) and differences in post processing and analyses. However, close localization of the abnormalities was observed in cingulate gyri of both hemispheres, left parahippocampal gyrus, postcentral gyrus, amygdala, and claustrum, right middle, and superior frontal gyri, temporal pole, and cerebellum. Interestingly, GM atrophy determined by VBM showed a closer anatomical relationship with reduced FC than surface measures by FreeSurfer; particularly in areas with GM reduction in the left hemisphere that correlated with increasing age in ASD patients (middle and superior temporal gyri, parahippocampus, and amygdala/uncus). These differences may be explained by the distinct methods for quantification used by VBM and FreeSurfer, which may also reflect different biological substrates between GM volume vs. cortical thinning and cortical areas as discussed above. Nevertheless, our results support the notion that brain alterations in high functioning autism, although subtle and diffuse, converge into areas of structural and functional changes of higher order multisensory association cortex (58). Also, the lack of close correlation between cortical thickness and FC patterns [as also found in other diseases (100)] indicate that changes in cortical thickness or GM atrophy that are not severe enough to be seen on routine MRIs, do not impact directly on FC patterns. This observation is in line with studies of brain networks showing that structural and functional network communities rarely overlap; i.e., functional modules are not always directly connected anatomically [for review see (153)].

LIMITATIONS

Limitations of our study include the potential effects of medication, a relatively small sample size that may have reduced statistical power and lack of information about puberty stages. However, the statistical significance of the results after correcting for multiple comparisons was remarkable. Our results cannot be generalized to younger and lower-functioning individuals with ASD since we studied a group that included only high functioning autism.

CONCLUSION

We found cortical thinning and diffuse GM reduction, more pronounced in the left hemisphere, as well as decreased FC between the left hemisphere and PCC (posterior aspect of the DMN) in patients with high-functioning autism. Reduced cortical thickness in the right inferior frontal lobe correlated with higher social impairment, while thinner cortices in the left precentral and superior frontal regions and thicker cortices in the right temporal pole and posterior cingulated correlated with greater communication impairment.

The combination of these abnormalities might represent a neurobiological pattern of this end of the spectrum of autism disorders, indicating a network disorder and could help explain some of the core behaviors in ASD. We also believe that new techniques, such as cortical thickness measurements and surface morphometry could help to elucidate in more detail the patterns of abnormalities related to age and the neurodevelopmental process.

AUTHOR CONTRIBUTIONS

AP and BC conducted data collection, data analyses and wrote the manuscript. AC, LP, TdR, IO, PD, and JdC contributed with study design and manuscript preparation and revision. J-CD contributed with study design, supervision, analyses of data, manuscript preparation and revision. FC contributed to study design and organization, supervision, funding, data analyses, manuscript preparation, and revision.

FUNDING

This study was supported by CNPq (Conselho Nacional de Desenvolvimento Científico e Tecnológico) and FAPESP (Fundação de Amparo à Pesquisa do Estado de São Paulo), grant # 2013/07559-3. Part of this work was performed within the framework of the Laboratory of Excellence LABEX ANR-11-LABEX-0042 of Université de Lyon, within the program Investissement d'Avenir (ANR-11-IDEX-0007) operated by the French National Research Agency (ANR).

ACKNOWLEDGMENTS

We are grateful to all individuals who underwent MRIs in this study for their helpful cooperation.

SUPPLEMENTARY MATERIAL

The Supplementary Material for this article can be found online at: https://www.frontiersin.org/articles/10.3389/fneur.2018.00539/full#supplementary-material

Supplementary Image 1 | Z-scored average connectivity maps of all seeds from both groups. With **(a)** we indicate controls' average maps, with **(b)**, patients' average maps. In (1), DMN maps, with seed on the posterior cingulated cortex; in (2) the seeds in the left temporal pole; in (3) with the seed on the left anterior hippocampus; in (4), with the seed on the left amygdala; in (5), the seed on the

interhemispheric medial frontal gyrus. The slices in (1), (2), and (5) were MNI axial: −32, −12, 18, 48, 78, and in (3) and (4) were MNI axial: −26, −12, 18, 48, 78.

Supplementary Image 2 | Areas of gray matter atrophy in voxel-based morphometry influenced by the age in patients with ASD. Gray matter atrophy determined by voxel-based morphometry, $p < 0.001$ clusters with at least 30 voxels.

Supplementary Image 3 | Inflated surface maps showing areas with increased and decrease cortical thickness in ASD compared to controls using ROI analysis. There was an increased thickness in right posterior cingulate (red), and in the right (green) and left lateral orbitofrontal cortex (blue) as well as decreased cortical thickness in the left paracentral (pink), posterior cingulate (yellow), and in the right temporal pole (orange) in the ASD group compared to controls.

REFERENCES

1. APA. *American Psychiatric Association; DSM-V development: Autism Spectrum Disorder* (2013). Available online at: http://www.dsm5.org/Documents/Autism%20Spectrum%20Disorder%20Fact%20Sheet.pdf
2. Baio J, Wiggins L, Christensen DL, Maenner MJ, Daniels J, Warren Z, et al. Prevalence of autism spectrum disorder among children aged 8 years — autism and developmental disabilities monitoring network, 11 sites, United States, 2014. *MMWR Surveill Summ.* (2018) 67:1–23. doi: 10.15585/mmwr.ss6706a1
3. Amaral DG, Schumann CM, Nordahl CW. Neuroanatomy of autism. *Trends Neurosci.* (2008) 31:137–45. doi: 10.1016/j.tins.2007.12.005
4. Bos DJ, Merchan-Naranjo J, Martinez K, Pina-Camacho L, Balsa I, Boada L, et al. Reduced gyrification is related to reduced interhemispheric connectivity in autism spectrum disorders. *J Am Acad Child Adolesc Psychiatry* (2015) 54:668–76. doi: 10.1016/j.jaac.2015.05.011
5. Ecker C, Ginestet C, Feng Y, Johnston P, Lombardo MV, Lai MC, et al. Brain surface anatomy in adults with autism: the relationship between surface area, cortical thickness, and autistic symptoms. *JAMA Psychiatry* (2013) 70:59–70. doi: 10.1001/jamapsychiatry.2013.265
6. Ecker C, Murphy D. Neuroimaging in autism–from basic science to translational research. *Nat Rev Neurol.* (2014) 10:82–91. doi: 10.1038/nrneurol.2013.276
7. Laird AR, Eickhoff SB, Kurth F, Fox PM, Uecker AM, Turner JA, et al. ALE meta-analysis workflows via the brainmap database: progress towards a probabilistic functional brain atlas. *Front Neuroinform.* (2009) 3:23. doi: 10.3389/neuro.11.023.2009
8. Libero LE, DeRamus TP, Lahti AC, Deshpande G, Kana RK. Multimodal neuroimaging based classification of autism spectrum disorder using anatomical, neurochemical, and white matter correlates. *Cortex* (2015) 66:46–59. doi: 10.1016/j.cortex.2015.02.008
9. Patriquin MA, DeRamus T, Libero LE, Laird A, Kana RK. Neuroanatomical and neurofunctional markers of social cognition in autism spectrum disorder. *Hum Brain Mapp.* (2016) 37:3957–78. doi: 10.1002/hbm.23288
10. Schaer M, Ottet MC, Scariati E, Dukes D, Franchini M, Eliez S, et al. Decreased frontal gyrification correlates with altered connectivity in children with autism. *Front Hum Neurosci.* (2013) 7:750. doi: 10.3389/fnhum.2013.00750
11. Via E, Radua J, Cardoner N, Happe F, Mataix-Cols D. Meta-analysis of gray matter abnormalities in autism spectrum disorder: should Asperger disorder be subsumed under a broader umbrella of autistic spectrum disorder? *Arch Gen Psychiatry* (2011) 68:409–18. doi: 10.1001/archgenpsychiatry.2011.27
12. Yu C, King BH. Focus on Autism and related conditions. *Focus* (2016) 14:3–8. doi: 10.1176/appi.focus.20150030
13. Hahamy A, Behrmann M, Malach R. The idiosyncratic brain: distortion of spontaneous connectivity patterns in autism spectrum disorder. *Nat Neurosci.* (2015) 18:302–9. doi: 10.1038/nn.3919
14. Supekar K, Uddin LQ, Prater K, Amin H, Greicius MD, Menon V. Development of functional and structural connectivity within the default mode network in young children. *Neuroimage* (2010) 52:290–301. doi: 10.1016/j.neuroimage.2010.04.009
15. Hull JV, Jacokes ZJ, Torgerson CM, Irimia A, Van Horn JD. Resting-state functional connectivity in autism spectrum disorders: a review. *Front Psychiatry* (2017) 7:205. doi: 10.3389/fpsyt.2016.00205
16. Minshew NJ, Williams DL. The new neurobiology of autism: cortex, connectivity, and neuronal organization. *Arch Neurol.* (2007) 64:945–50. doi: 10.1001/archneur.64.7.945
17. Aylward EH, Minshew NJ, Field K, Sparks BF, Singh N. Effects of age on brain volume and head circumference in autism. *Neurology* (2002) 59:175–83. doi: 10.1212/WNL.59.2.175
18. Nacewicz BM, Dalton KM, Johnstone T, Long MT, McAuliff EM, Oakes TR, et al. Amygdala volume and nonverbal social impairment in adolescent and adult males with autism. *Arch Gen Psychiatry* (2006) 63:1417–28. doi: 10.1001/archpsyc.63.12.1417
19. Keller TA, Kana RK, Just MA. A developmental study of the structural integrity of white matter in autism. *Neuroreport* (2007) 18:23–7. doi: 10.1097/01.wnr.0000239965.21685.99
20. Groen W, Teluij M, Buitelaar J, Tendolkar I. Amygdala and hippocampus enlargement during adolescence in autism. *J Am Acad Child Adolesc Psychiatry* (2010) 49:552–60. doi: 10.1016/j.jaac.2009.12.023
21. Saitoh O, Karns CM, Courchesne E. Development of the hippocampal formation from 2 to 42 years: MRI evidence of smaller area dentata in autism. *Brain* (2001) 124(Pt 7):1317–24. doi: 10.1093/brain/124.7.1317
22. McAlonan GM, Cheung V, Cheung C, Suckling J, Lam GY, Tai KS, et al. Mapping the brain in autism. A voxel-based MRI study of volumetric differences and intercorrelations in autism. *Brain* (2005) 128(Pt 2):268–76. doi: 10.1093/brain/awh332
23. Sears LL, Vest C, Mohamed S, Bailey J, Ranson BJ, Piven J. An MRI study of the basal ganglia in autism. *Prog Neuropsychopharmacol Biol Psychiatry* (1999) 23:613–24. doi: 10.1016/S0278–5846(99)00020-2
24. Langen M, Durston S, Staal WG, Palmen SJ, van Engeland H. Caudate nucleus is enlarged in high-functioning medication-naive subjects with autism. *Biol Psychiatry* (2007) 62:262–6. doi: 10.1016/j.biopsych.2006.09.040
25. Just MA, Cherkassky VL, Keller TA, Kana RK, Minshew NJ. Functional and anatomical cortical underconnectivity in autism: evidence from an fMRI study of an executive function task and corpus callosum morphometry. *Cereb Cortex* (2007) 17:951–61. doi: 10.1093/cercor/bhl006
26. Lefebvre A, Beggiato A, Bourgeron T, Toro R. Neuroanatomical diversity of corpus callosum and brain volume in autism: meta-analysis, analysis of the autism brain imaging data exchange project, and simulation. *Biol Psychiatry* (2015) 78:126–34. doi: 10.1016/j.biopsych.2015.02.010
27. Dajani DR, Uddin LQ. Local brain connectivity across development in autism spectrum disorder: A cross-sectional investigation. *Autism Res.* (2016) 9:43–54. doi: 10.1002/aur.1494
28. Cerliani L, Mennes M, Thomas RM, Di Martino A, Thioux M, Keysers C. Increased functional connectivity between subcortical and cortical resting-state networks in autism spectrum disorder. *JAMA Psychiatry* (2015) 72:767–77. doi: 10.1001/jamapsychiatry.2015.0101
29. Di Martino A, Yan CG, Li Q, Denio E, Castellanos FX, Alaerts K, et al. The autism brain imaging data exchange: towards a large-scale evaluation of the intrinsic brain architecture in autism. *Mol Psychiatry* (2014) 19:659–67. doi: 10.1038/mp.2013.78
30. Anderson JS, Nielsen JA, Froehlich AL, DuBray MB, Druzgal TJ, Cariello AN, et al. Functional connectivity magnetic resonance imaging classification of autism. *Brain* (2011) 134(Pt 12):3742–54. doi: 10.1093/brain/awr263
31. Anderson JS, Druzgal TJ, Froehlich A, DuBray MB, Lange N, Alexander AL, et al. Decreased interhemispheric functional connectivity in autism. *Cereb Cortex* (2011) 21:1134–46. doi: 10.1093/cercor/bhq190
32. Tyszka JM, Kennedy DP, Adolphs R, Paul LK. Intact bilateral resting-state networks in the absence of the corpus callosum. *J Neurosci.* (2011) 31:15154–62. doi: 10.1523/JNEUROSCI.1453-11.2011
33. Tyszka JM, Kennedy DP, Paul LK, Adolphs R. Largely typical patterns of resting-state functional connectivity in high-functioning adults with autism. *Cereb Cortex* (2013) 24(7):1894–905. doi: 10.1093/cercor/bht040

34. Uddin LQ. Idiosyncratic connectivity in autism: developmental and anatomical considerations. *Trends Neurosci.* (2015) 38:261–3. doi: 10.1016/j.tins.2015.03.004
35. Di Martino A, O'Connor D, Chen B, Alaerts K, Anderson JS, Assaf M, et al. Enhancing studies of the connectome in autism using the autism brain imaging data exchange II. *Sci Data* (2017) 4:170010. doi: 10.1038/sdata.2017.10
36. Byrge L, Dubois J, Tyszka JM, Adolphs R, Kennedy DP. Idiosyncratic brain activation patterns are associated with poor social comprehension in autism. *J Neurosci.* (2015) 35:5837–50. doi: 10.1523/JNEUROSCI.5182-14.2015
37. Ecker C, Bookheimer SY, Murphy DG. Neuroimaging in autism spectrum disorder: brain structure and function across the lifespan. *Lancet Neurol.* (2015) 14:1121–34. doi: 10.1016/S1474-4422(15)00050-2
38. Lenroot RK, Yeung PK. Heterogeneity within autism spectrum disorders: what have we learned from neuroimaging studies? *Front Hum Neurosci.* (2013) 7:733. doi: 10.3389/fnhum.2013.00733
39. Bauman ML, Kemper TL. Neuroanatomic observations of the brain in autism: a review and future directions. *Int J Dev Neurosci.* (2005) 23:183–7. doi: 10.1016/j.ijdevneu.2004.09.006
40. Courchesne E. Brain development in autism: early overgrowth followed by premature arrest of growth. *Ment Retard Dev Disabil Res Rev.* (2004) 10:106–11. doi: 10.1002/mrdd.20020
41. Courchesne E, Yeung-Courchesne R, Press GA, Hesselink JR, Jernigan TL. Hypoplasia of cerebellar vermal lobules VI and VII in autism. *N Engl J Med.* (1988) 318:1349–54. doi: 10.1056/NEJM198805263182102
42. Casanova MF, Buxhoeveden DP, Switala AE, Roy E. Minicolumnar pathology in autism. *Neurology* (2002) 58:428–32. doi: 10.1212/WNL.58.3.428
43. Li D, Karnath HO, Xu X. Candidate biomarkers in children with autism spectrum disorder: a review of MRI studies. *Neurosci Bull.* (2017) 33:219–37. doi: 10.1007/s12264-017-0118-1
44. Ecker C. The neuroanatomy of autism spectrum disorder: an overview of structural neuroimaging findings and their translatability to the clinical setting. *Autism* (2017) 21:18–28. doi: 10.1177/1362361315627136
45. Nickl-Jockschat T, Habel U, Michel TM, Manning J, Laird AR, Fox PT, et al. Brain structure anomalies in autism spectrum disorder–a meta-analysis of VBM studies using anatomic likelihood estimation. *Hum Brain Mapp.* (2012) 33:1470–89. doi: 10.1002/hbm.21299
46. Bonilha L, Cendes F, Rorden C, Eckert M, Dalgalarrondo P, Li LM, et al. Gray and white matter imbalance–typical structural abnormality underlying classic autism? *Brain Dev.* (2008) 30:396–401. doi: 10.1016/j.braindev.2007.11.006
47. Maximo JO, Keown CL, Nair A, Muller RA. Approaches to local connectivity in autism using resting state functional connectivity MRI. *Front Hum Neurosci.* (2013) 7:605. doi: 10.3389/fnhum.2013.00605
48. Dichter GS. Functional magnetic resonance imaging of autism spectrum disorders. *Dialog Clin Neurosci.* (2012) 14:319–51. Available online at: https://www.dialogues-cns.org/contents-14-3/dialoguesclinneurosci-14-319/
49. Belmonte MK, Allen G, Beckel-Mitchener A, Boulanger LM, Carper RA, Webb SJ. Autism and abnormal development of brain connectivity. *J Neurosci.* (2004) 24:9228–31. doi: 10.1523/JNEUROSCI.3340-04.2004
50. Just MA, Keller TA, Malave VL, Kana RK, Varma S. Autism as a neural systems disorder: a theory of frontal-posterior underconnectivity. *Neurosci Biobehav Rev.* (2012) 36:1292–313. doi: 10.1016/j.neubiorev.2012.02.007
51. Cherkassky VL, Kana RK, Keller TA, Just MA. Functional connectivity in a baseline resting-state network in autism. *Neuroreport* (2006) 17:1687–90. doi: 10.1097/01.wnr.0000239956.45448.4c
52. Kana RK, Libero LE, Hu CP, Deshpande HD, Colburn JS. Functional brain networks and white matter underlying theory-of-mind in autism. *Soc Cogn Affect Neurosci.* (2012) 9:98–105. doi: 10.1093/scan/nss106
53. Kennedy DP, Courchesne E. The intrinsic functional organization of the brain is altered in autism. *Neuroimage* (2008) 39:1877–85. doi: 10.1016/j.neuroimage.2007.10.052
54. Yerys BE, Gordon EM, Abrams DN, Satterthwaite TD, Weinblatt R, Jankowski KF, et al. Default mode network segregation and social deficits in autism spectrum disorder: evidence from non-medicated children. *Neuroimage Clin.* (2015) 9:223–32. doi: 10.1016/j.nicl.2015.07.018
55. Nebel MB, Joel SE, Muschelli J, Barber AD, Caffo BS, Pekar JJ, et al. Disruption of functional organization within the primary motor cortex in children with autism. *Hum Brain Mapp.* (2014) 35:567–80. doi: 10.1002/hbm.22188
56. Cheng W, Rolls ET, Gu H, Zhang J, Feng J. Autism: reduced connectivity between cortical areas involved in face expression, theory of mind, and the sense of self. *Brain* (2015) 138:1382–93. doi: 10.1093/brain/awv051
57. Ha S, Sohn IJ, Kim N, Sim HJ, Cheon KA. Characteristics of brains in autism spectrum disorder: structure, function and connectivity across the lifespan. *Exp Neurobiol.* (2015) 24:273–84. doi: 10.5607/en.2015.24.4.273
58. Mueller S, Keeser D, Samson AC, Kirsch V, Blautzik J, Grothe M, et al. Convergent findings of altered functional and structural brain connectivity in individuals with high functioning autism: a multimodal MRI study. *PLoS ONE* (2013) 8:e67329. doi: 10.1371/journal.pone.0067329
59. Chien HY, Lin HY, Lai MC, Gau SSF, Tseng WYI. Hyperconnectivity of the right posterior temporo-parietal junction predicts social difficulties in boys with autism spectrum disorder. *Autism Res.* (2015) 8:427–41. doi: 10.1002/aur.1457
60. Von Dem Hagen EAH, Stoyanova RS, Baron-Cohen S, Calder AJ. Reduced functional connectivity within and between "social" resting state networks in autism spectrum conditions. *Soc Cogn Affect Neurosci.* (2013) 8:694–701. doi: 10.1093/scan/nss053
61. Schilbach L, Eickhoff SB, Rotarska-Jagiela A, Fink GR, Vogeley K. Minds at rest? Social cognition as the default mode of cognizing and its putative relationship to the "default system" of the brain. *Conscious Cogn.* (2008) 17 457–67. doi: 10.1016/j.concog.2008.03.013.
62. Raichle ME, MacLeod AM, Snyder AZ, Powers WJ, Gusnard DA, Shulman GL. A default mode of brain function. *Proc Natl Acad Sci USA.* (2001) 98:676–682. doi: 10.1073/pnas.98.2.676
63. Müller R, Shih P, Keehn B. Underconnected, but how? A survey of functional connectivity MRI studies in autism spectrum disorders. *Cereb Cortex.* (2011) 21:2233–43. doi: 10.1093/cercor/bhq296
64. Lynch CJ, Uddin LQ, Supekar K, Khouzam A, Phillips J, Menon V. Default mode network in childhood autism: posteromedial cortex heterogeneity and relationship with social deficits. *Biol Psychiatry* (2013) 74:212–9. doi: 10.1016/j.biopsych.2012.12.013
65. Gilbert SJ, Williamson IDM, Dumontheil I, Simons JS, Frith CD, Burgess PW. Distinct regions of medial rostral prefrontal cortex supporting social and nonsocial functions. *Soc Cogn Affect Neurosci.* (2007) 2:217–26. doi: 10.1093/scan/nsm014
66. Baron-Cohen S. *Mindblindness: An Essay on Autism and Theory of Mind.* Cambridge, MA: MIT Press (1997).
67. Philip RCM, Dauvermann MR, Whalley HC, Baynham K, Lawrie SM, Stanfield AC. A systematic review and meta-analysis of the fMRI investigation of autism spectrum disorders. *Neurosci Biobehav Rev.* (2012) 36:901–42. doi: 10.1016/j.neubiorev.2011.10.008
68. Uddin LQ, Supekar K, Menon V. Typical and atypical development of functional human brain networks: insights from resting-state FMRI. *Front Syst Neurosci.* (2010) 4:21. doi: 10.3389/fnsys.2010.00021
69. Nomi JS, Uddin LQ. Developmental changes in large-scale network connectivity in autism. *Neuroimage Clin.* (2015) 7:732–41. doi: 10.1016/j.nicl.2015.02.024
70. Abrams DA, Lynch CJ, Cheng KM, Phillips J, Supekar K, Ryali S, et al. Underconnectivity between voice-selective cortex and reward circuitry in children with autism. *Proc Natl Acad Sci USA.* (2013) 110:12060–5. doi: 10.1073/pnas.1302982110
71. Fox MD, Snyder AZ, Vincent JL, Corbetta M, Van Essen DC, Raichle ME. The human brain is intrinsically organized into dynamic, anticorrelated functional networks. *Proc Natl Acad Sci USA.* (2005) 102:9673–8. doi: 10.1073/pnas.0504136102
72. Greicius MD, Krasnow B, Reiss AL, Menon V. Functional connectivity in the resting brain: a network analysis of the default mode hypothesis. *Proc Natl Acad Sci USA.* (2003) 100:253–8. doi: 10.1073/pnas.0135058100
73. Rosazza C, Minati L. Resting-state brain networks: literature review and clinical applications. *Neurol Sci.* (2011) 32:773–85. doi: 10.1007/s10072-011-0636-y
74. Biswal B, Yetkin FZ, Haughton VM, Hyde JS. Functional connectivity in the motor cortex of resting human brain using echo-planar MRI. *Magn Reson Med.* (1995) 34:537–41. doi: 10.1002/mrm.1910340409

75. Laughlin SB, Sejnowski TJ. Communication in neuronal networks. *Science* (2003) 301:1870–4. doi: 10.1126/science.1089662
76. Buckner RL, Andrews-Hanna JR, Schacter DL. The brain's default network: anatomy, function, and relevance to disease. *Ann N Y Acad Sci.* (2008) 1124:1–38. doi: 10.1196/annals.1440.011
77. Christoff K, Gordon AM, Smallwood J, Smith R, Schooler JW. Experience sampling during fMRI reveals default network and executive system contributions to mind wandering. *Proc Natl Acad Sci USA*. (2009) 106:8719–24. doi: 10.1073/pnas.0900234106
78. Mason MF, Norton MI, Van Horn JD, Wegner DM, Grafton ST, Macrae CN. Wandering minds: the default network and stimulus-independent thought. *Science* (2007) 315:393–5. doi: 10.1126/science.1131295
79. Raichle ME, Snyder AZ. A default mode of brain function: a brief history of an evolving idea. *Neuroimage* (2007) 37:1083–90, discussion 97–9. doi: 10.1016/j.neuroimage.2007.02.041
80. Damarla SR, Keller TA, Kana RK, Cherkassky VL, Williams DL, Minshew NJ, et al. Cortical underconnectivity coupled with preserved visuospatial cognition in autism: evidence from an fMRI study of an embedded figures task. *Autism Res.* (2010) 3:273–9. doi: 10.1002/aur.153
81. Geschwind DH, Levitt P. Autism spectrum disorders: developmental disconnection syndromes. *Curr Opin Neurobiol.* (2007) 17:103–11. doi: 10.1016/j.conb.2007.01.009
82. Washington SD, Gordon EM, Brar J, Warburton S, Sawyer AT, Wolfe A, et al. Dysmaturation of the default mode network in autism. *Hum Brain Mapp.* 35:1284–96. doi: 10.1002/hbm.22252
83. Mohammad-Rezazadeh I, Frohlich J, Loo SK, Jeste SS. Brain connectivity in autism spectrum disorder. *Curr Opin Neurol.* (2016) 29:137–47. doi: 10.1097/WCO.0000000000000301
84. Varcin KJ, Nelson CA III. A developmental neuroscience approach to the search for biomarkers in autism spectrum disorder. *Curr Opin Neurol.* (2016) 29:123–9. doi: 10.1097/WCO.0000000000000298
85. Mevel K, Fransson P, Bolte S. Multimodal brain imaging in autism spectrum disorder and the promise of twin research. *Autism* (2015) 19:527–41. doi: 10.1177/1362361314535510
86. Kana RK, Maximo JO, Williams DL, Keller TA, Schipul SE, Cherkassky VL, et al. Aberrant functioning of the theory-of-mind network in children and adolescents with autism. *Mol Autism* (2015) 6:59. doi: 10.1186/s13229-015-0052-x
87. Mahajan R, Mostofsky SH. Neuroimaging endophenotypes in autism spectrum disorder. *CNS Spectrums* (2015) 20:412–26. doi: 10.1017/S1092852915000371
88. Glerean E, Pan RK, Salmi J, Kujala R, Lahnakoski JM, Roine U, et al. Reorganization of functionally connected brain subnetworks in high-functioning autism. *Hum Brain Mapp.* (2016) 37:1066–79. doi: 10.1002/hbm.23084
89. Lord C, Rutter M, Le Couteur A. Autism diagnostic interview-revised: a revised version of a diagnostic interview for caregivers of individuals with possible pervasive developmental disorders. *J Autism Dev Disord.* (1994) 24:659–85. doi: 10.1007/BF02172145
90. Ashburner J, Friston KJ. Voxel-based morphometry–the methods. *Neuroimage* (2000) 11(6 Pt 1):805–21. doi: 10.1006/nimg.2000.0582
91. Ashburner J. A fast diffeomorphic image registration algorithm. *Neuroimage* (2007) 38:95–113. doi: 10.1016/j.neuroimage.2007.07.007
92. Fischl B, Dale AM. Measuring the thickness of the human cerebral cortex from magnetic resonance images. *Proc Natl Acad Sci USA*. (2000) 97:11050–5. doi: 10.1073/pnas.200033797
93. Fischl B, Sereno MI, Dale AM. Cortical surface-based analysis. II: Inflation, flattening, and a surface-based coordinate system. *Neuroimage* (1999) 9:195–207. doi: 10.1006/nimg.1998.0396
94. Dale AM, Fischl B, Sereno MI. Cortical surface-based analysis. I. Segmentation and surface reconstruction. *Neuroimage* (1999) 9:179–94. doi: 10.1006/nimg.1998.0395
95. Schaer M, Cuadra MB, Tamarit L, Lazeyras F, Eliez S, Thiran JP. A surface-based approach to quantify local cortical gyrification. *IEEE Trans Med Imaging* (2008) 27:161–70. doi: 10.1109/TMI.2007.903576
96. Zilles K, Armstrong E, Schleicher A, Kretschmann HJ. The human pattern of gyrification in the cerebral cortex. *Anat Embryol.* (1988) 179:173–9. doi: 10.1007/BF00304699
97. Hagler DJ, Jr., Saygin AP, Sereno MI. Smoothing and cluster thresholding for cortical surface-based group analysis of fMRI data. *Neuroimage* (2006) 33:1093–103. doi: 10.1016/j.neuroimage.2006.07.036
98. Desikan RS, Segonne F, Fischl B, Quinn BT, Dickerson BC, Blacker D, et al. An automated labeling system for subdividing the human cerebral cortex on MRI scans into gyral based regions of interest. *Neuroimage* (2006) 31:968–80. doi: 10.1016/j.neuroimage.2006.01.021
99. Fischl B, van der Kouwe A, Destrieux C, Halgren E, Segonne F, Salat DH, et al. Automatically parcellating the human cerebral cortex. *Cereb Cortex* (2004) 14:11–22. doi: 10.1093/cercor/bhg087
100. de Campos BM, Coan AC, Lin Yasuda C, Casseb RF, Cendes F. Large-scale brain networks are distinctly affected in right and left mesial temporal lobe epilepsy. *Hum Brain Mapp.* (2016) 37:3137–52. doi: 10.1002/hbm.23231
101. Lund TE, Norgaard MD, Rostrup E, Rowe JB, Paulson OB. Motion or activity: their role in intra- and inter-subject variation in fMRI. *Neuroimage* (2005) 26:960–4. doi: 10.1016/j.neuroimage.2005.02.021
102. Lowe MJ, Mock BJ, Sorenson JA. Functional connectivity in single and multislice echoplanar imaging using resting-state fluctuations. *Neuroimage* (1998) 7:119–32. doi: 10.1006/nimg.1997.0315
103. Franco AR, Mannell MV, Calhoun VD, Mayer AR. Impact of analysis methods on the reproducibility and reliability of resting-state networks. *Brain Connect*. (2013) 3:363–74. doi: 10.1089/brain.2012.0134
104. Zuo XN, Kelly C, Adelstein JS, Klein DF, Castellanos FX, Milham MP. Reliable intrinsic connectivity networks: test-retest evaluation using ICA and dual regression approach. *Neuroimage* (2010) 49:2163–77. doi: 10.1016/j.neuroimage.2009.10.080
105. Clemens B, Wagels L, Bauchmuller M, Bergs R, Habel U, Kohn N. Alerted default mode: functional connectivity changes in the aftermath of social stress. *Sci Rep*. (2017) 7:40180. doi: 10.1038/srep40180
106. Supekar K, Uddin LQ, Khouzam A, Phillips J, Gaillard WD, Kenworthy LE, et al. Brain hyperconnectivity in children with autism and its links to social deficits. *Cell Rep.* (2013) 5:738–47. doi: 10.1016/j.celrep.2013.10.001
107. Monk C, Peltier S, Wiggins J, Weng S. Abnormalities of intrinsic functional connectivity in autism spectrum disorders. *Neuroimage* (2009) 47:764–72. doi: 10.1016/j.neuroimage.2009.04.069
108. Kucharsky Hiess R, Alter R, Sojoudi S, Ardekani BA, Kuzniecky R, Pardoe HR. Corpus callosum area and brain volume in autism spectrum disorder: quantitative analysis of structural MRI from the ABIDE database. *J Autism Dev Disord*. (2015) 45:3107–14. doi: 10.1007/s10803-015-2468-8
109. Gori I, Giuliano A, Muratori F, Saviozzi I, Oliva P, Tancredi R, et al. Gray matter alterations in young children with autism spectrum disorders: comparing morphometry at the voxel and regional level. *J Neuroimag.* (2015) 25:866–74. doi: 10.1111/jon.12280
110. Richter J, Henze R, Vomstein K, Stieltjes B, Parzer P, Haffner J, et al. Reduced cortical thickness and its association with social reactivity in children with autism spectrum disorder. *Psychiatry Res.* (2015) 234:15–24. doi: 10.1016/j.pscychresns.2015.06.011
111. Jann K, Hernandez LM, Beck-Pancer D, McCarron R, Smith RX, Dapretto M, et al. Altered resting perfusion and functional connectivity of default mode network in youth with autism spectrum disorder. *Brain Behav*. (2015) 5:e00358. doi: 10.1002/brb3.358
112. Vissers ME, Cohen MX, Geurts HM. Brain connectivity and high functioning autism: a promising path of research that needs refined models, methodological convergence, and stronger behavioral links. *Neurosci Biobehav Rev*. (2012) 36:604–25. doi: 10.1016/j.neubiorev.2011.09.003
113. Erbetta A, Bulgheroni S, Contarino VE, Chiapparini L, Esposito S, Annunziata S, et al. Low-functioning autism and nonsyndromic intellectual disability: magnetic resonance imaging (MRI) findings. *J Child Neurol*. (2015) 30:1658–63. doi: 10.1177/0883073815578523
114. Katuwal GJ, Baum SA, Cahill ND, Michael AM. Divide and Conquer: Sub-Grouping of ASD Improves ASD Detection Based on Brain Morphometry. *PLoS ONE* (2016) 11:e0153331. doi: 10.1371/journal.pone.0153331
115. Machielsen WC, Rombouts SA, Barkhof F, Scheltens P, Witter MP. FMRI of visual encoding: reproducibility of activation. *Hum Brain Mapp.* (2000) 9:156–64. doi: 10.1002/(SICI)1097-0193(200003)9:33.0.CO;2-Q
116. Scheel C, Rotarska-Jagiela A, Schilbach L, Lehnhardt FG, Krug B, Vogeley K, et al. Imaging derived cortical thickness reduction in high-functioning

autism: key regions and temporal slope. *Neuroimage* (2011) 58:391–400. doi: 10.1016/j.neuroimage.2011.06.040
117. Hyde KL, Samson F, Evans AC, Mottron L. Neuroanatomical differences in brain areas implicated in perceptual and other core features of autism revealed by cortical thickness analysis and voxel-based morphometry. *Hum Brain Mapp*. 31:556–66. doi: 10.1002/hbm.20887
118. Wallace GL, Dankner N, Kenworthy L, Giedd JN, Martin A. Age-related temporal and parietal cortical thinning in autism spectrum disorders. *Brain* (2010) 133(Pt 12):3745–54. doi: 10.1093/brain/awq279
119. Herbert MR, Ziegler DA, Deutsch CK, O'Brien LM, Lange N, Bakardjiev A, et al. Dissociations of cerebral cortex, subcortical and cerebral white matter volumes in autistic boys. *Brain* (2003) 126(Pt 5):1182–92. doi: 10.1093/brain/awg110
120. Abrahams BS, Geschwind DH. Connecting genes to brain in the autism spectrum disorders. *Arch Neurol.* (2010) 67:395–9. doi: 10.1001/archneurol.2010.47
121. Hazlett HC, Poe MD, Gerig G, Smith RG, Piven J. Cortical gray and white brain tissue volume in adolescents and adults with autism. *Biol Psychiatry* (2006) 59:1–6. doi: 10.1016/j.biopsych.2005.06.015
122. Carper RA, Courchesne E. Localized enlargement of the frontal cortex in early autism. *Biol Psychiatry* (2005) 57:126–33. doi: 10.1016/j.biopsych.2004.11.005
123. Redcay E, Courchesne E. When is the brain enlarged in autism? A meta-analysis of all brain size reports. *Biol Psychiatry* (2005) 58:1–9. doi: 10.1016/j.biopsych.2005.03.026
124. Andrea M, Cathy JP, Karl JF, John A. Voxel-based morphometry of the human brain: methods and applications. *Curr Med Imag Rev*. (2005) 1:105–13. doi: 10.2174/1573405054038726
125. Ashburner J, Friston KJ. Why voxel-based morphometry should be used. *Neuroimage* (2001) 14:1238–43. doi: 10.1006/nimg.2001.0961
126. Schmitz N, Daly E, Murphy D. Frontal anatomy and reaction time in Autism. *Neurosci Lett*. (2007) 412:12–7. doi: 10.1016/j.neulet.2006.07.077
127. Hazlett HC, Poe MD, Gerig G, Styner M, Chappell C, Smith RG, et al. Early brain overgrowth in autism associated with an increase in cortical surface area before age 2 years. *Arch Gen Psychiatry* (2011) 68:467–76. doi: 10.1001/archgenpsychiatry.2011.39
128. Pontious A, Kowalczyk T, Englund C, Hevner RF. Role of intermediate progenitor cells in cerebral cortex development. *Dev Neurosci.* (2008) 30:24–32. doi: 10.1159/000109848
129. Wallace GL, Robustelli B, Dankner N, Kenworthy L, Giedd JN, Martin A. Increased gyrification, but comparable surface area in adolescents with autism spectrum disorders. *Brain* (2013) 136(Pt 6):1956–67. doi: 10.1093/brain/awt106
130. Chung MK, Robbins SM, Dalton KM, Davidson RJ, Alexander AL, Evans AC. Cortical thickness analysis in autism with heat kernel smoothing. *Neuroimage* (2005) 25:1256–65. doi: 10.1016/j.neuroimage.2004.12.052
131. Doyle-Thomas KA, Duerden EG, Taylor MJ, Lerch JP, Soorya LV, Wang AT, et al. Effects of age and symptomatology on cortical thickness in autism spectrum disorders. *Res Autism Spectrum Disord*. (2013) 7:141–50. doi: 10.1016/j.rasd.2012.08.004
132. Foster NE, Doyle-Thomas KA, Tryfon A, Ouimet T, Anagnostou E, Evans AC, et al. Structural gray matter differences during childhood development in autism spectrum disorder: a multimetric approach. *Pediatr Neurol*. (2015) 53:350–9. doi: 10.1016/j.pediatrneurol.2015.06.013
133. Dapretto M, Davies MS, Pfeifer JH, Scott AA, Sigman M, Bookheimer SY, et al. Understanding emotions in others: mirror neuron dysfunction in children with autism spectrum disorders. *Nat Neurosci.* (2006) 9:28–30. doi: 10.1038/nn1611
134. Kates WR, Ikuta I, Burnette CP. Gyrification patterns in monozygotic twin pairs varying in discordance for autism. *Autism Res.* (2009) 2:267–78. doi: 10.1002/aur.98
135. Assaf M, Jagannathan K, Calhoun VD, Miller L, Stevens MC, Sahl R, et al. Abnormal functional connectivity of default mode sub-networks in autism spectrum disorder patients. *Neuroimage* (2010) 53:247–56. doi: 10.1016/j.neuroimage.2010.05.067
136. Weng SJ, Wiggins JL, Peltier SJ, Carrasco M, Risi S, Lord C, et al. Alterations of resting state functional connectivity in the default network in adolescents with autism spectrum disorders. *Brain Res*. (2010) 1313:202–14. doi: 10.1016/j.brainres.2009.11.057
137. Tebartz van Elst L, Riedel A, Maier S. Autism as a disorder of altered global functional and structural connectivity. *Biol Psychiatry* (2016) 79:626–7. doi: 10.1016/j.biopsych.2016.02.003
138. Yahata N, Morimoto J, Hashimoto R, Lisi G, Shibata K, Kawakubo Y, et al. A small number of abnormal brain connections predicts adult autism spectrum disorder. *Nat Commun*. (2016) 7:11254. doi: 10.1038/ncomms11254
139. Rausch A, Zhang W, Haak KV, Mennes M, Hermans EJ, van Oort E, et al. Altered functional connectivity of the amygdaloid input nuclei in adolescents and young adults with autism spectrum disorder: a resting state fMRI study. *Mol Autism* (2016) 7:13. doi: 10.1186/s13229-015-0060-x
140. Jung M, Kosaka H, Saito DN, Ishitobi M, Morita T, Inohara K, et al. Default mode network in young male adults with autism spectrum disorder: relationship with autism spectrum traits. *Mol Autism* (2014) 5:35. doi: 10.1186/2040-2392-5-35
141. Olson IR, Plotzker A, Ezzyat Y. The Enigmatic temporal pole: a review of findings on social and emotional processing. *Brain* (2007) 130(Pt 7):1718–31. doi: 10.1093/brain/awm052
142. Gloor P. *The Temporal Lobe and Limbic System*. New York, NY: Oxford University Press (1997).
143. Irish M, Hodges JR, Piguet O. Right anterior temporal lobe dysfunction underlies theory of mind impairments in semantic dementia. *Brain* (2014) 137(Pt 4):1241–53. doi: 10.1093/brain/awu003
144. Baron-Cohen S, Leslie AM, Frith U. Does the autistic child have a "theory of mind"? *Cognition* (1985) 21:37–46. doi: 10.1016/0010-0277(85)90022-8
145. Blaizot X, Mansilla F, Insausti AM, Constans JM, Salinas-Alaman A, Pro-Sistiaga P, et al. The human parahippocampal region: I. Temporal pole cytoarchitectonic and MRI correlation. *Cereb Cortex* (2010) 20:2198–212. doi: 10.1093/cercor/bhp289
146. Frith U, Frith CD. Development and neurophysiology of mentalizing. *Philos Trans R Soc Lond Ser B Biol Sci*. (2003) 358:459–73. doi: 10.1098/rstb.2002.1218
147. Grezes J, Frith C, Passingham RE. Brain mechanisms for inferring deceit in the actions of others. *J Neurosci.* (2004) 24:5500–5. doi: 10.1523/JNEUROSCI.0219-04.2004
148. Heekeren HR, Wartenburger I, Schmidt H, Schwintowski HP, Villringer A. An fMRI study of simple ethical decision-making. *Neuroreport* (2003) 14:1215–9. doi: 10.1097/00001756-200307010-00005
149. Moll J, de Oliveira-Souza R, Eslinger PJ, Bramati IE, Mourao-Miranda J, Andreiuolo PA, et al. The neural correlates of moral sensitivity: a functional magnetic resonance imaging investigation of basic and moral emotions. *J Neurosci.* (2002) 22:2730–6. doi: 10.1523/JNEUROSCI.22-07-02730.2002
150. Vollm BA, Taylor AN, Richardson P, Corcoran R, Stirling J, McKie S, et al. Neuronal correlates of theory of mind and empathy: a functional magnetic resonance imaging study in a nonverbal task. *Neuroimage* (2006) 29:90–8. doi: 10.1016/j.neuroimage.2005.07.022
151. Rudie JD, Brown JA, Beck-Pancer D, Hernandez LM, Dennis EL, Thompson PM, et al. Altered functional and structural brain network organization in autism. *Neuroimage Clin*. (2013) 2:79–94. doi: 10.1016/j.nicl.2012.11.006
152. Honey CJ, Sporns O, Cammoun L, Gigandet X, Thiran JP, Meuli R, et al. Predicting human resting-state functional connectivity from structural connectivity. *Proc Natl Acad Sci USA*. (2009) 106:2035–40. doi: 10.1073/pnas.0811168106
153. Avena-Koenigsberger A, Misic B, Sporns O. Communication dynamics in complex brain networks. *Nat Rev Neurosci.* (2017) 19:17–33. doi: 10.1038/nrn.2017.149

Conflict of Interest Statement: The authors declare that the research was conducted in the absence of any commercial or financial relationships that could be construed as a potential conflict of interest.

Copyright © 2018 Pereira, Campos, Coan, Pegoraro, de Rezende, Obeso, Dalgalarrondo, da Costa, Dreher and Cendes. This is an open-access article distributed under the terms of the Creative Commons Attribution License (CC BY). The use, distribution or reproduction in other forums is permitted, provided the original author(s) and the copyright owner(s) are credited and that the original publication in this journal is cited, in accordance with accepted academic practice. No use, distribution or reproduction is permitted which does not comply with these terms.